U –Pb geochronology of zircons from river sediments in Sri Lanka: Implications on early Archean to late Cambrian magmatism and episodic crustal growth

Article · September 2018

DOI: 10.1016/j.jseaes.2018.08.029

11 authors, including:

Sanjeewa Malaviarachchi
University of Peradeniya
62 PUBLICATIONS **721** CITATIONS

P.L. Dharmapriya
University of Peradeniya
29 PUBLICATIONS **167** CITATIONS

Benxun Su
Chinese Academy of Sciences
153 PUBLICATIONS **2,584** CITATIONS

Chengli Zhang
Northwest University
58 PUBLICATIONS **1,465** CITATIONS

ARTICLE IN PRESS

Journal of Asian Earth Sciences xxx (xxxx) xxx–xxx

Contents lists available at ScienceDirect

Journal of Asian Earth Sciences

journal homepage: www.elsevier.com/locate/jseaes

Full length article

U-Pb geochronology of zircons from river sediments in Sri Lanka: Implications on early Archean to late Cambrian magmatism and episodic crustal growth

Sanjeewa P.K. Malaviarachchi[a,b,1,*], Subhashani Bindusara[a], Prasanna Lakshitha Dharmapriya[a], Ben-Can Su[c], Li Su[d], Ben-Xun Su[e], Hong Zhang[f], Chengli Zhang[f], Krishnan Sajeev[g], Patrick Asamoah Sakyi[h], Melesse Alemayehu[i,j]

[a] Department of Geology, Faculty of Science, University of Peradeniya, Peradeniya 20400, Sri Lanka
[b] Department of Geology, Faculty of Science, Niigata University, Ikarashi 950-2181, Japan
[c] PetroChina Co Ltd of Changqing Oilfield Company Eighth Oil Production Plant, Xi'an 710000, China
[d] Geological Lab Center, China University of Geosciences, Beijing 100083, China
[e] Key Laboratory of Mineral Resources, Institute of Geology and Geophysics, Chinese Academy of Sciences, Beijing 100029, China
[f] Key Laboratory of Continental Dynamics, Department of Geology, Northwest University, Xi'an, China
[g] Centre for Earth Science, Indian Institute of Science, Bangalore, India
[h] Department of Earth Science, School of Physical and Mathematical Sciences, University of Ghana, P.O. Box LG 58, Legon-Accra, Ghana
[i] School of Applied Natural Science, Applied Geology Department, Adama Science and Technology University, P.O. Box 1888, Adama, Ethiopia
[j] State Key Laboratory of Isotope Geochemistry, Guangzhou Institute of Geochemistry, Chinese Academy of Sciences, Guangzhou 510640, China

ARTICLE INFO

Keywords:
U–Pb geochronology
Gondwana
River sediment
Zircon
Sri Lanka

ABSTRACT

Geochronology of zircons from river-sediments in Sri Lanka has never been attempted. Here we present Rare Earth Elements (REE) and U-Pb isotopes of ~700 zircon grains by laser ablation ICP-MS technique, from sediments of the major rivers in the Sri Lankan basement (rivers of Mahaweli, Kelani, Kalu, Walawe, Maduru Oya and Maha Oya). Most of the studied zircons display oscillatory zoning and Th/U > 0.1, confirming their igneous origin. U-Pb age distribution of these river-sand zircons exhibits two major populations depicting Mesoproterozoic to Archean (~30%; > 1100–3100 Ma) and Neoproterozoic to late Cambrian (~70%; > 430–1000 Ma) magmatism. The two populations could be further resolved into intensive and episodic magmatic peaks at 480–680 Ma, 680–1000 Ma, 1100–1300 Ma, 1300–1700 Ma, 1700–1900 Ma, 2100–2300 Ma, 2300–2600 Ma and 2600–3100 Ma. These river-sediment-zircon data are consistent with the principal episodes of global continental crustal growth and the recognized U-Pb ages of magmatism are mostly correlative with those obtained from basement rocks by previous studies of Sri Lanka. The older zircons found in this study may have mainly originated from reworked/recycled ancient (Palaoproterozoic to Archean) crust. A younger zircon group of 450–700 Ma with homogenous core-rim zoning texture and Th/U ratios < 0.1 were inferred to be of metamorphic origin, indicating their possible crystallization at late Neoproterozoic metamorphic events, associated with the final assembly of the Gondwana Supercontinent. Thus, our data imply that the present-day continental crust of Sri Lanka may have predominantly formed and grown in the Neoproterozoic, while there is evidence that crustal growth began at least in the Paleoproterozoic. Further, the Mesoproterozoic peaks of the frequency distribution of U-Pb ages of river-sand zircons at ~1.6 Ga and ~1.1 Ga might reflect triggering of subduction in a paleo tectonic setting forming the Wanni and Vijayan dual arc systems, respectively.

1. Introduction

Accurate dating of rocks is very essential for unravelling major growth periods of the continental crust in the history of the Earth. However, the continental crust may have experienced long-term erosion and weathering whenever unroofed to the surface, so that most of

* Corresponding author at: Department of Geology, Faculty of Science, Niigata University, Ikarashi 950-2181, Japan.
E-mail addresses: malavi@pdn.ac.lk, sanjeewa@geo.sci.niigata-u.ac.jp (S.P.K. Malaviarachchi).
[1] Permanent address: Department of Geology, Faculty of Science, University of Peradeniya, Peradeniya 20400, Sri Lanka.

https://doi.org/10.1016/j.jseaes.2018.08.029
Received 12 March 2018; Received in revised form 28 August 2018; Accepted 28 August 2018
1367-9120/

Please cite this article as: Malaviarachchi, S.P.K., Journal of Asian Earth Sciences, https://doi.org/10.1016/j.jseaes.2018.08.029

the time all rock units were not well preserved. This perhaps, limits the opportunity for the entire rock succession to be successfully dated (e.g. Iizuka et al., 2005; Kemp et al., 2006; Rino et al., 2008; Hawkesworth et al., 2010, 2013; Condie et al., 2009, 2011). Thus, surveying of ages for all the rock units of a terrain is cumbersome and sometimes is very difficult in practice (Xu et al., 2016). However, zircon geochronology or 'zirconology', has been widely used to investigate provenance of terrains worldwide mainly due to the fact that zircon is a highly resistant mineral to weathering, produced by magmatic crystallization or as a result of metamorphic reactions. Thus, often zircons are entrapped in sedimentary rocks as 'detrital zircons', and commonly reworked in crust-mantle environments through multiple cycles. However, the U–Pb age would represent the formation of the original source rocks from which the zircon grains were derived (e.g. Amidon et al., 2005; Alizai et al., 2011; Su et al., 2011; Zheng et al., 2013; Deng et al., 2017). Therefore, in addition to routine dating of zircons in rocks, those separated from river sands are also utilized in several studies (e.g. Iizuka et al., 2005, 2013a,b; Rino et al., 2008; Yang et al., 2009; Wang et al., 2009, 2011a,b; Xu et al., 2016; Sakyi et al., 2018), since they may have preserved useful information for the age spectrum of the continental crust throughout the Earth's history.

The geology of the Sri Lankan basement is important to understand the tectonics of the Proterozoic to Cambrian Earth due to its close proximity to India, Madagascar and East Antarctica in the assembly of the Gondwana continent (e.g. Meert, 2003). Calc-silicate, Mg- and Al-rich meta-sedimentary, mafic to felsic meta-igneous and high- to ultra high-temperature granulites together with amphibolites, migmatites, minor gabbroic, granitic, pegmatitic and aplitic igneous intrusions characterize the Sri Lankan basement (Cooray, 1994 and references therein). Therefore, this tectonic amalgamation of amphibolite to granulite-facies terrains with igneous intercalations consisting of diverse geochemical signatures in a small area within the Sri Lankan terrain attracts great interest in the fields of petrology, geochronology and structural geology.

Despite many previous studies on zirconology of the basement rocks of Sri Lanka, the provenance, evolutionary history and the U–Pb isotope systematics of individual detrital zircon grains from the Sri Lankan river systems have never been attempted. Therefore, we present a synthesis of U-Pb age data on various zircons sampled from major rivers in the Sri Lankan Precambrian basement (rivers of Mahaweli, Kelani, Kalu, Walawe, Maduru Oya and Maha Oya). These zircons show two major populations depicting wide-spread magmatism dated as Mesoproterozoic to Archean and Neoproterozoic to late Cambrian, evidencing episodic crustal growth in the Sri Lankan basement.

2. Geological outline

The Sri Lankan Precambrian basement has been subdivided into four major terrains (e.g. Cooray, 1994), namely: the Highland (HC), Wanni (WC), Vijayan (VC) and Kadugannawa (KC) complexes (Fig. 1), based on Nd isotope model age mapping and zircon geochronology (Milisenda et al., 1988, 1994; Kröner et al., 1987, 1991). The WC occupies a higher crustal level than the HC although there is no clear structural break between the rocks of the two complexes; probably the contact has been obliterated by later events (Voll and Kleinschrodt, 1991). The boundary between the VC and the HC is well defined as a thrust/shear contact (Hatherton et al., 1975; Vitanage, 1985; Voll and Kleinschrodt, 1991; Kriegsman, 1995). Three tectonic klippens with petrological and structural features similar to the HC are exposed in the southeastern part of Sri Lanka as inliers, namely Kataragama Klippe, Buttala Klippe and Kuda Oya Klippe. The HC domain is interpreted to be a part of a supracrustal basin developed in a suture zone with Lützow-Holm Complex in East Antarctica at the last phase of Gondwana assembly (Shiraishi et al., 1994). The KC is in contact with the WC and the HC. The WC, KC and VC domains were originated in Grenville-age arc-related settings (Kröner et al., 2003; Willbold et al., 2004; Kröner et al., 2013).

2.1. Lithological characteristics

The HC is made up of granulitic meta-quartzites, marbles, calcsilicates and metapelitic gneisses, intimately associated with charnockites (Cooray, 1962, 1984; Mathavan and Fernando, 2001). Meta-sedimentary rocks such as marble and quartzite could be traced for more than 40 km in the central and northeastern parts of the HC, while marble and quartzite in the southwestern parts of the HC are scarce (Mathavan et al., 1999). Bands of wollastonite, diopside- and scapolite-bearing granulites and cordierite-bearing gneisses mainly occur in the south and south western parts of the HC (Cooray, 1962, 1984; Hapuarachchi, 1968; Mathavan et al., 1999; Perera, 1984; Prame, 1991). Typical high temperature (granulite facies) metamorphic conditions are well established for the HC from meta-basaltic and gabbroic to intermediate rocks (Sandiford et al., 1988; Schumacher et al., 1990), charnockites and metamorphosed pelitic rocks (Perera, 1984, 1987; Prame, 1991, Hiroi et al., 1994, Raase and Schenk, 1994; Dharmapriya et al., 2016, 2017; Fernando et al., 2017).

The HC granulites have been subjected to a folding and thrusting event after the peak metamorphic conditions (Berger and Jayasinghe, 1976; Kriegsman, 1995; Kleinschrodt, 1994). The large folds with wavelengths of about 7–10 km and an exposed length parallel to their axes up to 50 km in the central Highlands were formed at slightly lower temperatures (700–750 °C) than the peak metamorphism (800–850 °C, 8–9 kbar) and hence the deformation has ended at granulite facies conditions (Kleinschrodt, 1994). Hiroi et al. (2014) reported evidence for fast exhumation of lower-crustal rocks to andalusite-stable upper-crustal conditions by channel flow in a continental collision orogeny, based on felsic inclusions (granitic inclusions) within high grade ordinary granulites and UHT granulites of the HC.

The WC occurs northwest and west of the HC and is consists predominantly of upper amphibolite to granulite facies meta-igneous gneisses and minor meta-sediments. The predominant meta-igneous rocks show a vast range of protolith-chemistry from granitic, granodioritic, monzonitic, tonalitic, charnockitic and enderbitic compositions (e.g., Pohl and Emmermann, 1991). Garnet sillimanite gneisses, cordierite gneisses, quartzites and calc-silicate rocks occur as minor meta-sediments, close to the inferred boundary with the HC. The western part of the WC is mainly composed of less-deformed granites.

The KC is a set of doubly plunging synforms, cropping out in the northwestern part of Kandy. It comprises upper amphibolite to granulite facies basement rocks (Kröner et al., 1991; Cooray, 1994). Relics of primary magmatic layering are preserved in these synforms mainly composed of hornblende gneisses, amphibolites and minor pyroxenites (Kröner et al., 1991). Hornblende- and biotite-bearing ortho gneissic rocks are of calc-alkaline origin with gabbroic, dioritic and trondhjemitic compositions, interlayered with granodioritic to granitic gneisses, charnockites, enderbites and minor meta-sediments (Kröner et al., 2003).

The VC is exposed in eastern Sri Lanka and consists predominantly of meta-igneous rocks, which are upper amphibolite-facies calc-alkaline granitoid gneisses including augen-gneisses, with minor amphibolite layers possibly derived from mafic dykes. This granitoid suite was interpreted as a product of subduction-related magmatism (Pohl and Emmermann, 1991). The granitoid gneisses show TTG-dominated I-type signatures (Milisenda, 1991; Pohl and Emmermann, 1991), while the hornblende gneisses display compositions between diorite and leucogranite with the dominant compositions being granodiorite and granite (Kröner et al., 1991; Milisenda, 1991; Kleinschrodt, 1994; Milisenda et al., 1994).

2.2. Previous geochronology

Ion microprobe U-Pb study on zircons by Kröner et al. (1987) documented late Archean to Paleoproterozoic ages (3.2–2.4 Ga) for detrital grains from the HC meta-sediments. Also, they reported an

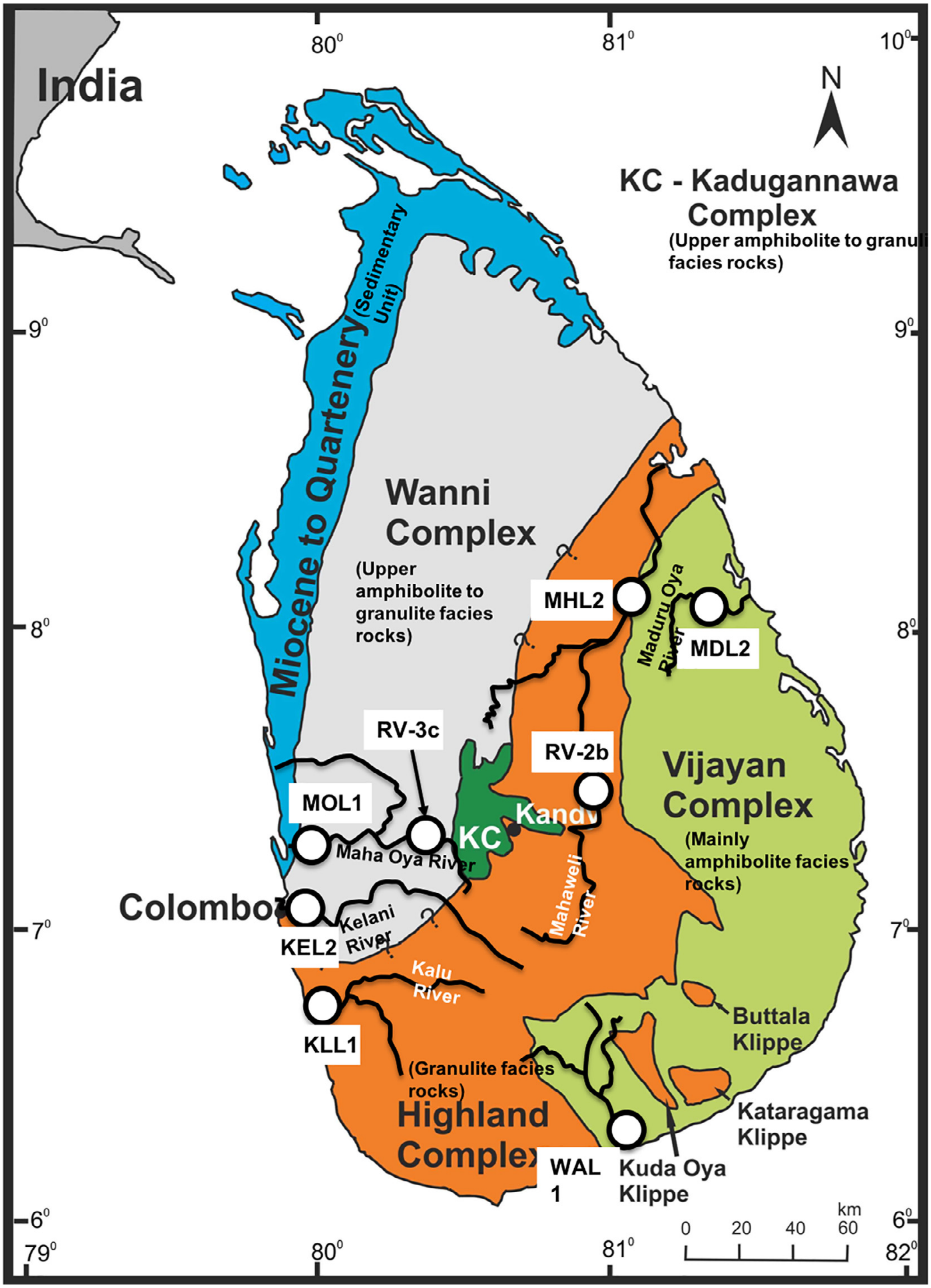

Fig. 1. Simplified geologic map of Sri Lanka (after Cooray, 1994), showing river-sand sample localities of the major river basins of Sri Lanka, namely: Mahaweli, Kelani, Kalu, Walawe, Maha Oya and Maduru Oya Rivers. Sample numbers are: Mahaweli (MHL2, RV-2b), Kelani (KEL2), Kalu (KLL1), Walawe (WAL1), Maha Oya (MOL1, RV-3c) and Maduru Oya (MDL2).

intrusion age of 1.1 Ga and new zircon growth at about 550 Ma in meta-igneous rocks. Milisenda et al. (1988) found Nd isotope model ages for the HC at 3.0–2.2 Ga, indicating the HC was derived from late Archean sources. Köhler et al. (1991) and Baur et al. (1991) reported U-Pb zircon crystallization ages of 1940 Ma and a Pb loss event at 560–550 Ma, indicating that high grade metamorphism. Kröner and Williams (1993) reported SHRIMP zircon ages for granitic gneiss from the HC as 1.9 Ga for the crystallization of the igneous protolith and 531 Ma as the age of metamorphism. Malaviarachchi and Takasu (2011) obtained ages of ~728–460 Ma from monazite.

The WC has Nd isotope modal ages of ca. 700–1.1 Ga and shows a wide spectrum of magmatic events as documented by zircon ages of 1100–530 Ma (Burton and O'Nions, 1990; Kröner et al., 1991, 2003). Massive charnockites from north of the WC have protolith emplacement ages of ~1 Ga Ma determined from zircon evaporation method (Kröner et al., 1994). Deposition of detrital zircons in meta-pelites and the

Table 1
Sample locations of zircons in Sri Lankan river sands.

River	Sample no.	Location	Coordinates
Mahaweli	MHL2 (n = 72)	Manampitiya	7.9121° N, 81.0899° E
	RV-2b (n = 88)	Mahiyangana	7.3312° N, 80.9880° E
Kelani	KEL2 (n = 88)	Sedawatta	6.9540° N, 79.8827° E
Kalu	KLL1 (n = 112)	Kaluthara	6.5922° N, 79.9657° E
Walawe	WAL1 (n = 88)	Ambalantota	6.1063° N, 81.0158° E
Maduru Oya	MDL2 (n = 85)	Aralaganwila	7.7577° N, 81.1776° E
Maha Oya	MOL1 (n = 50)	Kochchikade	7.2710° N, 79.8654° E
	RV3c (n = 75)	Alawwa	7.2942° N, 80.2420° E

emplacement of magmatic zircons of charnockitic and enderbitic rocks yielded ion microprobe U-Pb concordia upper intercept ages of ~1.1 Ga as their precursor protolith timings. The respective lower intercept ages range between 540 and 590 Ma, reflecting high-grade metamorphism.

Nd-model ages of the rocks from the KC range between ~900 Ma and 1.6 Ga (Milisenda et al., 1988, 1994). Pb-Pb zircon evaporation ages for the KC yielded ~770 Ma – 1.1 Ga, indicating multiple calc-alkaline magmatic activities, covering a period of approx. 300 Ma (Kröner et al., 2003; Willbold et al., 2004). Most of the dioritic to granodioritic rocks of the KC display ca. 900 Ma ages. Xenomorphic zircons of gabbroic gneisses yielded relatively younger ages of ~700 Ma while idiomorphic zircons from the same sample gave ages of ~900 Ma (Kröner et al., 2003; Willbold et al., 2004).

Milisenda et al. (1988, 1994) reported whole-rock Nd isotope analyses of the VC rocks and found a mean crustal residence ages of 1.0–1.8 Ga. These authors also found that their Sr isotope data are in line with the Nd isotope results, suggesting that the majority of the VC rocks were juvenile and derived from a typical LREE-depleted, mantle-derived precursor and not from anatexis of older crustal lithologies (Milisenda et al., 1988, 1994; Kröner et al., 1991). Rb–Sr whole-rock isochron ages of ~800 Ma by De Maesschalck et al. (1990) were ascribed to metamorphic resetting. Magmatic zircons reflect emplacement of the protoliths of the Vijayan gneisses at 1000–1100 Ma (Kröner et al., 2013).

3. Methodology

Heavy mineral separation from river sand samples was performed at the Department of Geology, Faculty of Science, University of Peradeniya. Zircons were further refined by gravimetric methods and finally handpicked at Indian Institute of Science, Bangalore, India. The separated zircons from six samples (MHL2, KEL2, KLL1, WAL1, MOL1 and MDL2) were then mounted in epoxy resins and polished down to near half sections at the Institute of Geology and Geophysics, Chinese Academy of Sciences (IGGCAS), Beijing, China. The internal structure of zircons was studied with a NOVA NanoSEM scanning electron microscope at IGGCAS. U-Pb dating of the above-mentioned six samples was carried out using LA-ICPMS at the China University of Geoscience, Beijing, following analytical procedures described in Song et al. (2005, 2010). The laser ablation instrument couples a quadrupole ICP-MS (Agilient 7500a) and a UP-193 Solid-State laser (193 nm, New Wave Research Inc.) with the automatic positioning system. For the present work, laser spot size was set to ~36 μm for most analyses and to 25 μm for metamorphic rims, laser energy density at 8.5 J/cm2 and repetition rate at 10 Hz. The procedure of laser sampling is 5-s pre-ablation, 20-s sample-chamber flushing and 40-s sampling ablation. The ablated material is carried into the ICP-MS by the high-purity Helium gas stream with flux of 0.8 L/min. The whole laser path was fluxed with N2 (15 L/min) and Ar (1.15 L/min) in order to increase energy stability. The counting time for U, Th, ^{204}Pb, ^{206}Pb, ^{207}Pb and ^{208}Pb is 20 ms, and is 15 ms for other elements. Calibrations for the zircon analyses were carried out using NIST 610 glass as an external standard and Si as internal standard. U–Pb isotope fractionation effects were corrected using zircon 91,500 (Wiedenbeck et al., 1995) as external standard. Zircon standard TEMORA (417 Ma) from Australia (Black et al., 2003) is also used as a secondary standard to supervise the deviation of age measurement/calculation.

Samples RV-2b and RV-3c were mounted in epoxy resins and polished down to near half sections to expose internal structures, and then analyzed at Key Laboratory of Continental Dynamics, Northwest University in Xi'an, using a Geolas 193 nm laser ablation system coupled with an Agilent 7700x mass spectrometer using analytical procedures of Yuan et al. (2004). Using a combination of cathodoluminescence (CL) and optical microscopy, the zircon crystals with the internal structure were selected as suitable targets for laser ablation analyses. Laser ablation was operated at a constant energy 60 mJ and a repetition rate of 6 Hz, with a spot diameter of 30 μm, using external standards of 91,500 and NIST 612 for U-Pb age and trace elements, respectively.

Isotopic ratios and element concentrations of zircons were calculated using GLITTER (ver. 4.4, Macquarie University). Concordia ages and diagrams were obtained using Isoplot/Ex (3.0) (Ludwig, 2003). The common Pb was corrected using LA-ICP-MS Common Lead Correction (ver. 3.15), followed the method of Andersen (2002). All the quoted age uncertainties are at 2 sigma level.

4. Samples

In the present work, we contribute new data on Rare Earth Elements (REE) and U–Pb ages of zircons in sand from the major rivers of Sri Lanka. The data included in this paper come from the Mahaweli (MHL2, RV-2b), Kelani (KEL2), Kalu (KLL1), Walawe (WAL1), Maha Oya (MOL1, RV-3c) and Maduru Oya (MDL2) rivers in Sri Lanka (Table 1; Fig. 1). These rivers drain a large area covering more than half of the Sri Lankan continental block. Also, the large catchment area of these rivers located in the core portions of all the litho-tectonic units of Sri Lanka is composed of high-grade metamorphic rocks. The zircon grains from six rivers were investigated for morphology, REE analysis and U-Pb dating. Most of the analyzed zircons are euhedral to subhedral in shape, colorless to dark, and range in size from 25 to 400 μm, where most zircons (~80–85%) display oscillatory zoning patterns implying their magmatic origin (Fig. 2). Metamorphic zircons appear in CL images as more-or-less homogeneous and/or have overgrowth rims on detrital cores, constituting up to ca. 15–20% of total grains studied.

5. Results

The zircon grains from the six rivers were analyzed for morphology, REE and U-Pb isotopes. U-Pb age data are tabulated in the Table 2 and REE are given in Supplementary Tables 1–6. The CL images of representative zircon grains are shown in Figs. 2 and 3. Approximately 100 spots in zircon from each river were analyzed for U/Pb ages and only those with discordance < 10% were considered for age data interpretations. The results are displayed graphically for each river in concordia diagrams and U–Pb age histograms (Figs. 4–6). Th/U vs. age is plotted in the Fig. 7 and chondrite-normalized REE plots are shown in Fig. 8. From the grains which plot off the U–Pb concordia curve, a true discordant age was not obtained, because the zircons may be mutually unrelated in their genesis. The results used for age interpretations here are only from grains with > 90% concordance. Further, we used ^{207}Pb/^{206}Pb ages for the zircon grains with age > 1.0 Ga and ^{206}Pb/^{238}U ages for those < 1.0 Ga.

Most of the zircon grains from the Mahaweli River are rounded to elongated and subhedral-anhedral in shape. These grains are big in size and vary from 150 to 400 μm in length. They show oscillatory zoning, core–rim texture and homogeneous appearance in CL images (Fig. 3a). One hundred and eighty eight spots on 160 grains were analyzed. Grains younger than ~700 Ma closely plot on the concordia line (Fig. 4a). Zircon data from the Mahaweli River show a prominent peak at 560 Ma and minor peaks from 730 to 2450 Ma (Fig. 5a, g).

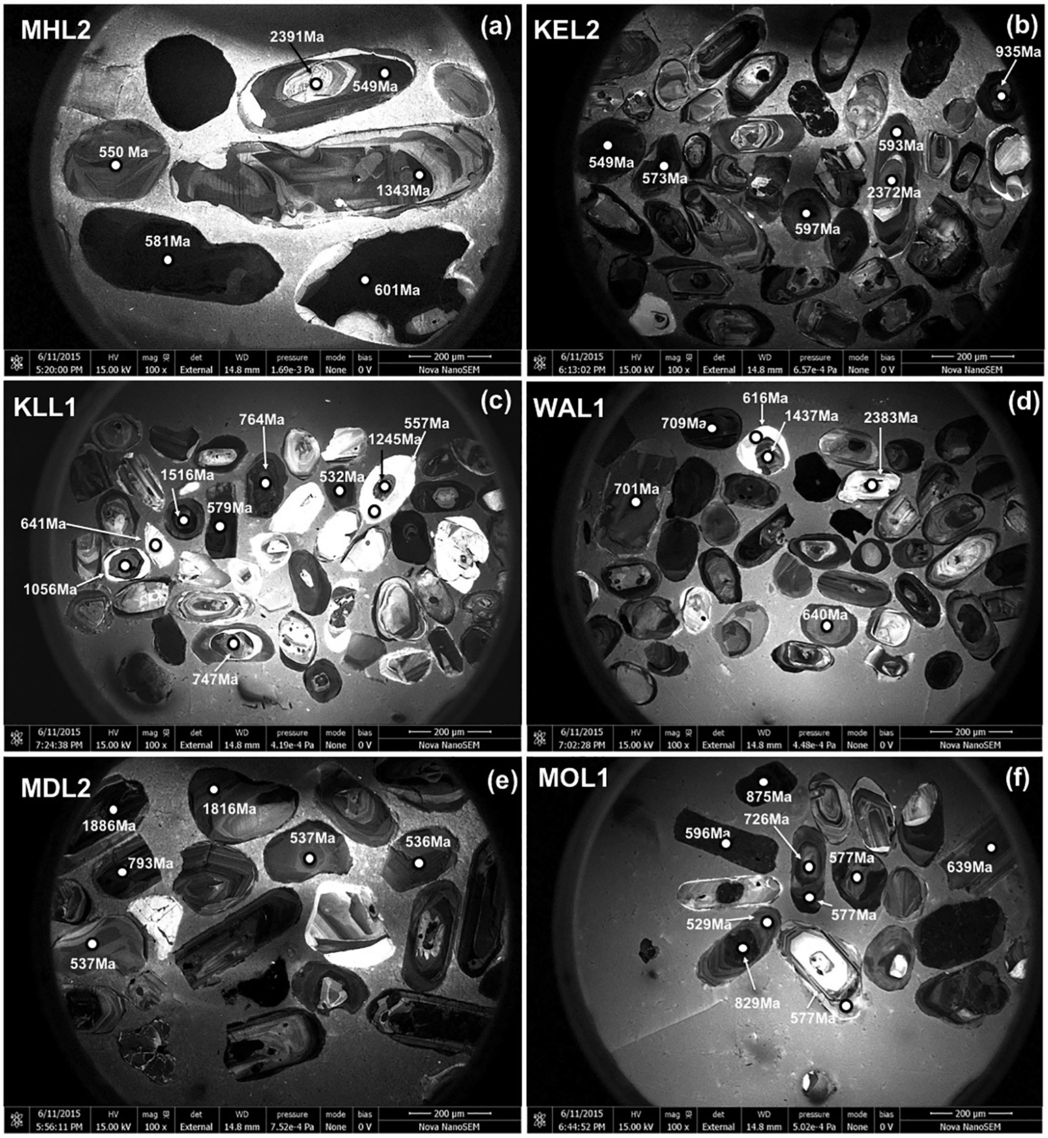

Fig. 2. Cathodoluminescence (CL) images of the studied zircons from the major river basins of Sri Lanka. Representative age data (analytical spot is marked with a circle) are also noted on the grains. Magmatic zircons are characterized by clear oscillatory zoning while, metamorphic grains are homogeneous and/or have core-rim zones/overgrowths peculiar to different age populations. See text for details. Sample numbers are same as those in Fig. 1.

The zircon grains from the Kelani River are rounded to elongated and subhedral-anhedral in shape. These grains vary from 50 to 250 µm in size. They show oscillatory zoning, core–rim texture and homogeneous appearance in CL images (Fig. 3b). Ninety-eight spots on 88 grains were analyzed. Grains younger than ~1 Ga closely plot on the concordia line (Fig. 4b). Zircons from the Kelani River show two major peaks at 530 and 560 Ma, together with significant multiple peaks from 660 to 2300 Ma (Fig. 5b).

From the Kalu River, most of the zircon grains are rounded to elongated and subhedral to anhedral in shape. These grains are relatively small and vary from 25 to 200 µm in size. They show oscillatory zoning, core–rim texture and homogeneous appearance in CL images (Fig. 5c). One hundred and twenty spots on 112 grains were analyzed. Grains younger than ~700 Ma closely plot on the concordia line (Fig. 4c). Interestingly, zircons of Kalu River display five major peaks from 550 to 930 Ma together with some minor peaks staring from 460 Ma to 2200 Ma.

Rounded to elongated and subhedral to anhedral zircons were observed in the Walawe River sample. These grains vary from 50- to 200 µm in size. They show oscillatory zoning, core–rim texture and homogeneous appearance in CL images (Fig. 3d). One hundred spots on 88 grains were analysed. Grains younger than ~800 Ma and as old as ~2 Ga closely plot on the Concordia line. Further, these grains define a clear Discordia line as well, with a lower and upper intercept of ~600 Ma and 1.8 Ga, respectively (Fig. 4d). Zircons from the Walawe River are characterized with a major peak shooting at 570–605 Ma along with characteristic composite peaks from 1250 to 2100 Ma and subordinate peaks at 470, 700 and 870 Ma (Fig. 5d).

The Maduru Oya samples contain zircons rounded to elongated and subhedral to anhedral in shape. These grains are relatively small and vary from 100 to 400 µm in size. They show oscillatory zoning, core–rim texture and homogeneous appearance in CL images (Fig. 3e). One hundred spots on 85 grains were analyzed. Grains younger than ~1 and ~1.8 Ga closely plot on the concordia line (Fig. 4e). The Maduru Oya is characterized by a clear peak at ~550–580 Ma, while having subordinate peaks in the range of 460–2600 Ma (Fig. 5e).

Obtained zircon grains from the Maha Oya are rounded to elongated and subhedral to anhedral in shape. These grains are relatively small and vary from 50 to 200 µm in size. They show oscillatory zoning, core–rim texture and homogeneous appearance in CL images (Fig. 3f).

Table 2
Measured U-Pb isotope ratios and age data of the river sand zircon from Sri Lanka.

River	Analysis (Sample No. and Spot No.)	CORRECTED RATIOS $^{207}Pb/^{206}Pb$	1σ	$^{207}Pb/^{235}U$	1σ	$^{206}Pb/^{238}U$	1σ	$^{208}Pb/^{232}Th$	1σ	CORRECTED AGES (Ma) $^{207}Pb/^{206}Pb$	1σ	$^{207}Pb/^{235}U$	1σ	$^{206}Pb/^{238}U$	1σ	$^{208}Pb/^{232}Th$	1σ	Degree of Discordance	Th/U
Mahaweli	**MHL2-01**	0.05491	0.00196	0.69040	0.02417	0.09117	0.00124	0.02703	0.00066	409	54	533	15	562	7	539	12	5.16%	0.44
	MHL2-02	0.05857	0.00132	0.71575	0.01574	0.08861	0.00114	0.02653	0.00060	551	26	548	9	547	7	529	29	0.18%	0.36
	MHL2-03	0.11466	0.00132	5.13048	0.05834	0.32445	0.00387	0.08989	0.00114	1875	10	1841	10	1811	19	1740	29	3.53%	0.71
	MHL2-05	0.05870	0.00075	0.76740	0.00967	0.09480	0.00113	0.02708	0.00039	556	12	578	6	584	7	540	13	1.03%	0.28
	MHL2-06	0.05860	0.00079	0.77394	0.01030	0.09577	0.00115	0.02756	0.00043	552	13	582	6	590	7	550	11	1.36%	0.24
	MHL2-07	0.05919	0.00410	0.73326	0.05015	0.08983	0.00149	0.02591	0.00056	574	10	558	29	555	9	517	12	0.54%	1.78
	MHL2-08	0.05801	0.00120	0.72913	0.01469	0.09114	0.00117	0.02668	0.00042	530	23	556	9	562	7	532	20	1.07%	0.80
	MHL2-09	0.05852	0.00084	0.75587	0.01058	0.09367	0.00113	0.02714	0.00036	549	14	572	6	577	7	541	6	0.87%	0.93
	MHL2-10	0.05805	0.00120	0.73644	0.01478	0.09200	0.00117	0.02718	0.00044	532	23	560	9	567	7	542	22	1.23%	0.69
	MHL2-11	0.06039	0.00120	0.81702	0.01305	0.09812	0.00116	0.03028	0.00035	618	44	606	7	603	7	603	5	0.50%	0.17
	MHL2-12	0.06025	0.00081	0.91132	0.01196	0.10967	0.00132	0.03128	0.00083	613	13	658	6	671	8	623	10	1.94%	0.05
	MHL2-13	0.05830	0.00079	0.77355	0.01028	0.09621	0.00116	0.02735	0.00043	541	13	582	6	592	7	545	10	1.69%	0.23
	MHL2-16	0.11361	0.00127	5.55319	0.06165	0.35443	0.00420	0.09144	0.00120	1858	10	1909	10	1956	20	1769	14	5.01%	0.26
	MHL2-17	0.06032	0.00106	0.84259	0.01102	0.10131	0.00118	0.03127	0.00037	615	39	621	6	622	7	622	25	0.16%	0.07
	MHL2-18	0.05982	0.00071	0.81574	0.00956	0.09888	0.00117	0.03080	0.00047	597	12	606	5	608	7	613	52	0.33%	0.11
	MHL2-19	0.05861	0.01187	0.70889	0.14184	0.08771	0.00304	0.02816	0.00169	553	43	544	84	542	18	561	15	0.37%	1.03
	MHL2-20	0.05946	0.01375	0.74330	0.17007	0.09065	0.00331	0.02672	0.00188	584	34	564	99	559	20	533	15	0.89%	1.01
	MHL2-21	0.05917	0.01340	0.72649	0.16327	0.08902	0.00277	0.02908	0.00197	573	42	554	96	550	16	579	17	0.73%	0.95
	MHL2-22	0.05899	0.00253	0.73260	0.03087	0.09005	0.00130	0.02715	0.00059	567	66	558	18	556	8	541	10	0.36%	0.89
	MHL2-24	0.05769	0.00109	0.72358	0.01340	0.09095	0.00114	0.02719	0.00040	518	20	553	8	561	7	542	14	1.43%	0.91
	MHL2-25	0.05825	0.00151	0.74630	0.01894	0.09291	0.00122	0.02768	0.00054	539	33	566	11	573	7	552	15	1.22%	0.54
	MHL2-27	0.05883	0.00167	0.73771	0.02042	0.09092	0.00121	0.02869	0.00055	561	37	561	12	561	7	572	11	0.00%	0.63
	MHL2-29	0.05937	0.00079	0.87391	0.01147	0.10674	0.00128	0.02978	0.00045	581	13	638	6	654	7	593	12	2.45%	0.26
	MHL2-30	0.11652	0.00171	5.74205	0.08179	0.35734	0.00450	0.09768	0.00157	1904	11	1938	12	1970	21	1884	14	3.35%	0.67
	MHL2-32	0.05771	0.00162	0.67227	0.01843	0.08446	0.00113	0.02734	0.00048	519	37	522	11	523	7	545	16	0.19%	0.77
	MHL2-33	0.05824	0.00214	0.70477	0.02543	0.08775	0.00123	0.02672	0.00072	539	54	542	15	542	7	533	13	0.00%	0.55
	MHL2-34	0.05823	0.00108	0.72509	0.01319	0.09029	0.00113	0.02820	0.00048	538	20	554	8	557	7	562	25	0.54%	0.45
	MHL2-35	0.05790	0.00186	0.72457	0.02269	0.09074	0.00126	0.02511	0.00094	526	44	553	13	560	7	501	18	1.25%	0.37
	MHL2-37	0.05881	0.00094	0.78841	0.01231	0.09721	0.00119	0.02770	0.00111	560	16	590	7	598	7	552	9	1.34%	0.07
	MHL2-39	0.05834	0.00133	0.72541	0.01620	0.09016	0.00115	0.02710	0.00129	543	27	554	10	556	7	540	19	0.36%	0.11
	MHL2-40	0.05962	0.00099	0.78731	0.01278	0.09575	0.00118	0.02792	0.00054	590	17	590	7	589	7	557	43	0.17%	0.27
	MHL2-43	0.05902	0.00080	0.87299	0.01164	0.10726	0.00129	0.02999	0.00053	568	13	637	6	657	8	597	10	3.04%	0.15
	MHL2-44	0.05777	0.00204	0.69242	0.02394	0.08691	0.00124	0.02718	0.00062	521	51	534	14	537	7	542	33	0.56%	0.64
	MHL2-45	0.05789	0.00245	0.70314	0.02931	0.08807	0.00126	0.02732	0.00068	526	66	541	17	544	7	545	20	0.55%	0.61
	MHL2-46	0.05915	0.00570	0.76338	0.07274	0.09358	0.00182	0.02845	0.00075	573	15	576	42	577	11	567	14	0.17%	2.02
	MHL2-47	0.05559	0.00118	0.71519	0.01473	0.09328	0.00122	0.02746	0.00048	436	24	548	9	575	7	548	23	4.70%	0.81
	MHL2-48	0.05828	0.00158	0.72230	0.01912	0.08986	0.00120	0.02651	0.00061	540	35	552	11	555	7	529	12	0.54%	0.49
	MHL2-49	0.16040	0.00203	10.22051	0.12748	0.46203	0.00559	0.11652	0.00169	2460	10	2455	12	2449	25	2228	13	0.45%	0.57
	MHL2-50	0.06216	0.00172	0.79730	0.02154	0.09301	0.00124	0.02576	0.00053	680	35	595	12	573	7	514	19	3.84%	0.61
	MHL2-51	0.05934	0.00176	0.74546	0.02157	0.09110	0.00124	0.02671	0.00059	580	39	566	13	562	7	533	19	0.71%	0.64
	MHL2-52	0.11072	0.00142	4.80724	0.06055	0.31484	0.00380	0.08381	0.00126	1811	10	1786	11	1764	19	1627	19	2.66%	0.27
	MHL2-54	0.05822	0.00102	0.74054	0.01261	0.09224	0.00115	0.02658	0.00046	538	18	563	7	569	7	530	15	1.05%	0.47
	MHL2-57	0.05894	0.00090	0.81571	0.01224	0.10035	0.00123	0.02855	0.00057	565	15	606	7	616	7	569	30	1.62%	0.15
	MHL2-58	0.05896	0.00097	0.78328	0.01259	0.09633	0.00119	0.02808	0.00068	566	16	587	7	593	7	560	30	1.01%	0.13
	MHL2-59	0.05937	0.00081	0.88009	0.01178	0.10749	0.00130	0.03030	0.00055	581	13	641	6	658	8	603	13	2.58%	0.09
	MHL2-60	0.06181	0.00182	0.84404	0.02256	0.09905	0.00123	0.03048	0.00076	667	65	621	12	609	7	607	16	1.97%	0.12
	MHL2-61	0.05855	0.00104	0.77112	0.01332	0.09550	0.00119	0.02790	0.00045	550	18	580	8	588	7	556	11	1.36%	0.79
	MHL2-64	0.05852	0.00085	0.85308	0.01210	0.10571	0.00129	0.02922	0.00052	549	14	626	7	648	8	582	21	3.40%	0.15
	MHL2-67	0.05992	0.00086	0.86559	0.01221	0.10475	0.00128	0.02942	0.00052	601	14	633	7	642	7	586	18	1.40%	0.14

(*continued on next page*)

Table 2 (*continued*)

River	Analysis (Sample No. and Spot No.)	CORRECTED RATIOS $^{207}Pb/^{206}Pb$	1σ	$^{207}Pb/^{235}U$	1σ	$^{206}Pb/^{238}U$	1σ	$^{208}Pb/^{232}Th$	1σ	CORRECTED AGES (Ma) $^{207}Pb/^{206}Pb$	1σ	$^{207}Pb/^{235}U$	1σ	$^{206}Pb/^{238}U$	1σ	$^{208}Pb/^{232}Th$	1σ	Degree of Discordance	Th/U
	MHL2-68	0.06534	0.00098	1.02132	0.01492	0.11335	0.00139	0.04404	0.00080	785	14	715	7	692	8	871	22	3.32%	0.13
	MHL2-69	0.05956	0.00109	0.73180	0.01308	0.08910	0.00112	0.02629	0.00047	588	19	558	8	550	7	525	13	1.45%	0.53
	MHL2-70	0.05870	0.00096	0.75002	0.01198	0.09265	0.00115	0.02553	0.00044	556	16	568	7	571	7	510	17	0.53%	0.41
	MHL2-71	0.05814	0.00163	0.68826	0.01887	0.08584	0.00116	0.02572	0.00052	535	37	532	11	531	7	513	9	0.19%	0.78
	MHL2-72	0.05779	0.00242	0.72469	0.02975	0.09093	0.00133	0.02790	0.00073	522	64	553	18	561	8	556	18	1.43%	0.63
	MHL2-75	0.05884	0.00122	0.74627	0.01507	0.09197	0.00119	0.02712	0.00047	561	23	566	9	567	7	541	14	0.18%	1.07
	MHL2-76	0.05881	0.00160	0.73619	0.01947	0.09077	0.00123	0.02646	0.00056	560	34	560	11	560	7	528	36	0.00%	0.67
	MHL2-78	0.05794	0.00096	0.85321	0.01375	0.10678	0.00133	0.02815	0.00056	527	16	626	8	654	8	561	9	4.28%	0.22
	MHL2-79	0.06029	0.00104	0.84448	0.01417	0.10157	0.00127	0.02810	0.00059	614	17	622	8	624	7	560	11	0.32%	0.22
	MHL2-80	0.05868	0.00130	0.76666	0.01645	0.09474	0.00124	0.02741	0.00057	555	25	578	9	584	7	547	18	1.03%	0.51
	MHL2-81	0.05864	0.00090	0.75503	0.01130	0.09336	0.00115	0.02715	0.00044	554	15	571	7	575	7	541	2	0.70%	0.70
	MHL2-84	0.05877	0.00138	0.78425	0.01796	0.09676	0.00127	0.02839	0.00055	559	28	588	10	595	7	566	14	1.18%	0.74
	MHL2-85	0.06135	0.00128	0.90176	0.01528	0.10660	0.00130	0.03284	0.00039	652	46	653	8	653	8	653	5	0.00%	0.11
	MHL2-88	0.06179	0.00118	0.92103	0.01363	0.10811	0.00130	0.03327	0.00087	667	42	663	7	662	8	662	8	0.15%	0.01
	MHL2-89	0.06132	0.00125	0.89002	0.01454	0.10527	0.00127	0.03243	0.00039	650	45	646	8	645	7	645	12	0.16%	0.08
	MHL2-90	0.05813	0.00743	0.72321	0.09151	0.09022	0.00207	0.02634	0.00148	535	14	553	54	557	12	525	9	0.72%	0.77
	MHL2-92	0.05989	0.00213	0.70010	0.02324	0.08478	0.00110	0.02619	0.00038	600	79	539	14	525	7	522	7	2.67%	0.27
	MHL2-94	0.06050	0.00097	0.80224	0.01255	0.09615	0.00119	0.02813	0.00053	622	16	598	7	592	7	561	7	1.01%	0.14
	MHL2-95	0.05887	0.00140	0.72074	0.01671	0.08878	0.00116	0.02748	0.00062	562	28	551	10	548	7	548	9	0.55%	0.32
	MHL2-96	0.05911	0.00096	0.76749	0.01213	0.09415	0.00117	0.02406	0.00045	571	16	578	7	580	7	481	10	0.34%	0.18
	RV-2b-92	0.07055	0.00098	1.09690	0.01268	0.11274	0.00080	0.04184	0.00041	945	28	752	6	689	5	829	8	9.18%	0.29
	RV-2b-93	0.06840	0.00130	0.97435	0.01672	0.10330	0.00082	0.05437	0.00117	881	39	691	9	634	5	1070	22	8.99%	0.08
	RV-2b-64	0.06724	0.00223	0.93512	0.02949	0.10084	0.00110	0.02722	0.00110	845	67	670	15	619	6	543	22	8.24%	0.16
	RV-2b-79	0.06640	0.00104	0.90702	0.01238	0.09906	0.00073	0.06045	0.00091	819	33	656	7	609	4	1186	17	7.65%	0.09
	RV-2b-39	0.07489	0.00170	1.46548	0.03083	0.14188	0.00127	0.04925	0.00082	1066	45	916	13	855	7	972	16	7.13%	0.36
	RV-2b-54	0.06895	0.00241	1.09280	0.03658	0.11494	0.00132	0.04120	0.00085	897	71	750	18	701	8	816	17	6.93%	0.56
	RV-2b-36	0.06374	0.00344	0.78696	0.04110	0.08953	0.00140	0.02923	0.00189	733	27	589	23	553	8	582	37	6.64%	0.16
	RV-2b-84	0.06255	0.00090	0.72150	0.00878	0.08365	0.00059	0.02916	0.00033	693	30	552	5	518	4	581	7	6.51%	0.20
	RV-2b-94	0.07494	0.00210	1.55273	0.04120	0.15026	0.00154	0.04402	0.00073	1067	55	952	16	902	9	871	14	5.45%	0.72
	RV-2b-24	0.06477	0.00176	0.89564	0.02291	0.10027	0.00095	0.04479	0.00103	767	56	649	12	616	6	886	20	5.42%	0.19
	RV-2b-56	0.07544	0.00281	1.60095	0.05731	0.15390	0.00192	0.04774	0.00106	1080	73	971	22	923	11	943	20	5.18%	0.67
	RV-2b-57	0.06379	0.00181	0.85243	0.02281	0.09691	0.00094	0.03610	0.00083	735	59	626	13	596	6	717	16	4.98%	0.25
	RV-2b-35	0.06630	0.00102	1.02364	0.01364	0.11195	0.00083	0.04840	0.00082	816	32	716	7	684	5	955	16	4.62%	0.09
	RV-2b-04	0.06160	0.00383	0.74429	0.04496	0.08761	0.00152	0.02712	0.00136	660	23	565	26	541	9	541	27	4.34%	0.31
	RV-2b-34	0.06117	0.00317	0.72111	0.03620	0.08548	0.00125	0.02706	0.00084	645	22	551	21	529	7	540	16	4.27%	0.53
	RV-2b-30	0.06182	0.00229	0.76372	0.02712	0.08957	0.00100	0.02677	0.00051	668	11	576	16	553	6	534	10	4.20%	0.75
	RV-2b-72	0.07377	0.00226	1.53880	0.04479	0.15127	0.00165	0.04758	0.00074	1035	61	946	18	908	9	940	14	4.17%	0.98
	RV-2b-52	0.06928	0.00107	1.23694	0.01660	0.12947	0.00096	0.04449	0.00043	907	32	818	8	785	5	880	8	4.15%	0.49
	RV-2b-32	0.16787	0.00221	10.23509	0.11269	0.44210	0.00358	0.11946	0.00168	2537	22	2456	10	2360	16	2281	30	7.48%	0.31
	RV-2b-107	0.06622	0.00242	1.04290	0.03655	0.11421	0.00133	0.03364	0.00082	813	75	725	18	697	8	669	16	4.06%	0.48
	RV-2b-104	0.06135	0.00288	0.74110	0.03369	0.08760	0.00117	0.02724	0.00068	651	46	563	20	541	7	543	13	4.01%	0.65
	RV-2b-77	0.07044	0.00275	1.33380	0.05009	0.13730	0.00176	0.04143	0.00075	941	78	861	22	829	10	821	15	3.75%	1.14
	RV-2b-09	0.06080	0.00091	0.73390	0.00949	0.08753	0.00064	0.03307	0.00056	632	32	559	6	541	4	658	11	3.31%	0.08
	RV-2b-13	0.11104	0.00172	4.62326	0.06268	0.30190	0.00251	0.09066	0.00100	1817	28	1754	11	1701	12	1754	19	6.81%	0.64
	RV-2b-110	0.07147	0.00197	1.43672	0.03754	0.14578	0.00147	0.04184	0.00068	971	55	904	16	877	8	828	13	3.09%	0.70
	RV-2b-66	0.11267	0.00189	4.81343	0.07191	0.30979	0.00268	0.09164	0.00100	1843	30	1787	13	1740	13	1772	18	5.93%	0.92
	RV-2b-71	0.10923	0.00184	4.50761	0.06727	0.29923	0.00256	0.08515	0.00109	1787	30	1732	12	1688	13	1652	20	5.87%	0.60
	RV-2b-82	0.11331	0.00161	4.89158	0.05881	0.31304	0.00244	0.08815	0.00084	1853	25	1801	10	1756	12	1708	16	5.55%	0.77
	RV-2b-51	0.06048	0.00140	0.74425	0.01607	0.08924	0.00076	0.02846	0.00094	621	49	565	9	551	5	567	18	2.50%	0.08
	RV-2b-83	0.11261	0.00189	4.83775	0.07233	0.31153	0.00269	0.08969	0.00114	1842	30	1792	13	1748	13	1736	21	5.37%	0.60

(*continued on next page*)

Table 2 (*continued*)

River	Analysis (Sample No. and Spot No.)	CORRECTED RATIOS								CORRECTED AGES (Ma)									
		$^{207}Pb/^{206}Pb$	1σ	$^{207}Pb/^{235}U$	1σ	$^{206}Pb/^{238}U$	1σ	$^{208}Pb/^{232}Th$	1σ	$^{207}Pb/^{206}Pb$	1σ	$^{207}Pb/^{235}U$	1σ	$^{206}Pb/^{238}U$	1σ	$^{208}Pb/^{232}Th$	1σ	Degree of Discordance	Th/U
	RV-2b-101	0.07225	0.00307	1.52629	0.06257	0.15319	0.00212	0.04819	0.00150	993	84	941	25	919	12	951	29	2.42%	0.43
	RV-2b-95	0.07368	0.00223	1.62795	0.04694	0.16022	0.00172	0.04773	0.00109	1033	60	981	18	958	10	942	21	2.41%	0.42
	RV-2b-67	0.07259	0.00149	1.56094	0.02938	0.15592	0.00133	0.04830	0.00049	1003	41	955	12	934	7	953	10	2.22%	1.13
	RV-2b-05	0.10737	0.00130	4.39322	0.04272	0.29671	0.00217	0.08344	0.00073	1755	22	1711	8	1675	11	1620	14	4.79%	0.48
	RV-2b-108	0.11175	0.00215	4.81995	0.08481	0.31276	0.00295	0.08869	0.00123	1828	34	1788	15	1754	14	1717	23	4.21%	0.71
	RV-2b-78	0.06731	0.00119	1.22273	0.01936	0.13174	0.00102	0.04085	0.00049	847	36	811	9	798	6	809	10	1.65%	0.43
	RV-2b-43	0.06231	0.00231	0.89506	0.03182	0.10416	0.00118	0.03152	0.00106	685	77	649	17	639	7	627	21	1.63%	0.25
	RV-2b-58	0.05977	0.00133	0.73600	0.01523	0.08931	0.00074	0.02661	0.00109	595	48	560	9	551	4	531	21	1.58%	0.06
	RV-2b-109	0.05994	0.00332	0.74927	0.04036	0.09065	0.00138	0.02655	0.00105	601	56	568	23	559	8	530	21	1.50%	0.39
	RV-2b-81	0.05917	0.00146	0.70293	0.01618	0.08615	0.00075	0.02775	0.00066	573	53	541	10	533	4	553	13	1.46%	0.18
	RV-2b-99	0.05828	0.00156	0.64918	0.01643	0.08077	0.00074	0.02588	0.00061	540	58	508	10	501	4	516	12	1.46%	0.22
	RV-2b-85	0.06414	0.00130	1.02677	0.01910	0.11608	0.00095	0.03545	0.00051	746	42	717	10	708	5	704	10	1.31%	0.38
	RV-2b-41	0.07022	0.00303	1.44819	0.06027	0.14955	0.00205	0.04263	0.00083	935	86	909	25	899	11	844	16	1.18%	1.22
	RV-2b-29	0.05942	0.00193	0.73027	0.02261	0.08911	0.00091	0.02601	0.00033	583	69	557	13	550	5	519	6	1.16%	1.40
	RV-2b-75	0.06787	0.00178	1.28590	0.03178	0.13740	0.00131	0.04302	0.00046	865	54	840	14	830	7	851	9	1.16%	1.64
	RV-2b-86	0.07119	0.00163	1.52850	0.03242	0.15569	0.00140	0.04598	0.00065	963	46	942	13	933	8	909	12	0.98%	0.63
	RV-2b-73	0.07143	0.00212	1.54742	0.04368	0.15710	0.00166	0.04705	0.00124	970	59	950	17	941	9	929	24	0.95%	0.30
	RV-2b-74	0.06386	0.00214	1.03360	0.03313	0.11737	0.00127	0.03821	0.00107	737	69	721	17	715	7	758	21	0.74%	0.29
	RV-2b-40	0.07160	0.00142	1.57225	0.02852	0.15923	0.00133	0.04875	0.00091	975	40	959	11	953	7	962	18	0.71%	0.23
	RV-2b-91	0.07477	0.00249	1.82033	0.05797	0.17656	0.00207	0.05101	0.00091	1062	66	1053	21	1048	11	1006	17	1.35%	0.92
	RV-2b-80	0.06020	0.00215	0.80953	0.02769	0.09752	0.00106	0.04221	0.00884	611	75	602	16	600	6	836	15	0.38%	0.01
	RV-2b-76	0.06988	0.00177	1.46665	0.03496	0.15219	0.00144	0.04364	0.00054	925	51	917	14	913	8	863	11	0.38%	1.10
	RV-2b-33	0.06901	0.00132	1.40783	0.02453	0.14793	0.00121	0.04280	0.00048	899	39	892	10	889	7	847	9	0.33%	0.72
	RV-2b-06	0.05949	0.00239	0.76766	0.02964	0.09357	0.00113	0.02785	0.00074	585	85	578	17	577	7	555	14	0.31%	0.45
	RV-2b-08	0.11022	0.00166	4.87027	0.06413	0.32042	0.00264	0.10692	0.00106	1803	27	1797	11	1792	13	2053	19	0.63%	0.74
	RV-2b-105	0.05943	0.00158	0.77931	0.01954	0.09509	0.00086	0.02878	0.00055	583	57	585	11	586	5	574	11	0.07%	0.34
	RV-2b-23	0.11284	0.00141	5.19813	0.05253	0.33403	0.00247	0.09116	0.00078	1846	22	1852	9	1858	12	1763	15	0.66%	0.65
	RV-2b-27	0.11232	0.00180	5.15059	0.07302	0.33250	0.00283	0.09454	0.00107	1837	29	1845	12	1851	14	1826	20	0.71%	0.73
	RV-2b-12	0.05814	0.00251	0.70726	0.02947	0.08821	0.00109	0.03192	0.00128	534	92	543	18	545	6	635	25	0.35%	0.19
	RV-2b-88	0.06604	0.00256	1.24359	0.04629	0.13656	0.00170	0.03935	0.00779	808	79	821	21	825	10	780	4	0.57%	0.02
	RV-2b-02	0.05813	0.00119	0.71641	0.01347	0.08937	0.00073	0.02652	0.00027	534	45	549	8	552	4	529	5	0.60%	0.82
	RV-2b-11	0.06159	0.00117	0.94438	0.01627	0.11118	0.00089	0.03480	0.00058	660	40	675	9	680	5	692	11	0.65%	0.21
	RV-2b-100	0.05684	0.00182	0.63804	0.01946	0.08140	0.00080	0.02461	0.00058	485	70	501	12	505	5	491	11	0.67%	0.32
	RV-2b-62	0.05885	0.00108	0.77068	0.01265	0.09496	0.00073	0.02963	0.00052	562	39	580	7	585	4	590	10	0.79%	0.17
	RV-2b-17	0.06678	0.00237	1.32319	0.04502	0.14366	0.00166	0.04340	0.00108	831	72	856	20	865	9	859	21	1.09%	0.44
	RV-2b-25	0.05727	0.00713	0.69061	0.08472	0.08744	0.00221	0.03198	0.00557	501	56	533	51	540	13	636	9	1.33%	0.13
	RV-2b-55	0.06885	0.00294	1.49274	0.06157	0.15724	0.00217	0.04565	0.00143	894	86	927	25	941	12	902	28	1.49%	0.44
	RV-2b-96	0.05710	0.00528	0.68816	0.06247	0.08739	0.00181	0.02525	0.00101	495	12	532	38	540	11	504	20	1.56%	0.86
	RV-2b-59	0.05720	0.00172	0.69464	0.01986	0.08807	0.00085	0.04407	0.00232	499	65	536	12	544	5	872	45	1.56%	0.04
	RV-2b-45	0.05712	0.00166	0.69680	0.01927	0.08845	0.00084	0.02671	0.00076	496	64	537	12	546	5	533	15	1.74%	0.19
	RV-2b-03	0.05710	0.00126	0.70133	0.01442	0.08907	0.00075	0.02660	0.00040	495	49	540	9	550	4	531	8	1.89%	0.38
	RV-2b-16	0.05698	0.00227	0.70054	0.02695	0.08915	0.00103	0.02618	0.00077	490	86	539	16	551	6	522	15	2.07%	0.35
	RV-2b-10	0.05651	0.00192	0.69685	0.02266	0.08942	0.00094	0.02880	0.00163	472	74	537	14	552	6	574	32	2.75%	0.07
	RV-2b-60	0.05616	0.00301	0.70163	0.03670	0.09060	0.00121	0.02561	0.00087	459	45	540	22	559	7	511	17	3.45%	0.41
	RV-2b-49	0.06521	0.00538	1.43239	0.11595	0.15928	0.00346	0.03893	0.00275	781	65	903	48	953	19	772	53	5.28%	0.37
Kelani	**KEL2-01**	0.05987	0.00108	0.74731	0.01345	0.09051	0.00104	0.02679	0.00046	599	20	567	8	559	6	534	9	1.43%	0.22
	KEL2-02	0.07023	0.00163	1.09705	0.02206	0.11330	0.00131	0.03437	0.00038	935	49	752	11	692	8	683	7	8.67%	0.11
	KEL2-03	0.06036	0.00110	0.83132	0.01509	0.09987	0.00115	0.03718	0.00064	617	20	614	8	614	7	738	12	0.00%	0.19
	KEL2-04	0.05790	0.00131	0.68698	0.01535	0.08603	0.00104	0.02581	0.00058	526	28	531	9	532	6	515	11	0.19%	0.30
	KEL2-05	0.06175	0.00203	0.79125	0.02413	0.09293	0.00115	0.02860	0.00037	666	72	592	14	573	7	570	7	3.32%	0.10

(continued on next page)

Table 2 (*continued*)

River	Analysis (Sample No. and Spot No.)	CORRECTED RATIOS								CORRECTED AGES (Ma)									
		$^{207}Pb/^{206}Pb$	1σ	$^{207}Pb/^{235}U$	1σ	$^{206}Pb/^{238}U$	1σ	$^{208}Pb/^{232}Th$	1σ	$^{207}Pb/^{206}Pb$	1σ	$^{207}Pb/^{235}U$	1σ	$^{206}Pb/^{238}U$	1σ	$^{208}Pb/^{232}Th$	1σ	Degree of Discordance	Th/U
	KEL2-06	0.16392	0.00318	9.81822	0.18791	0.43432	0.00537	0.12298	0.00218	2497	17	2418	18	2325	24	2344	39	7.40%	1.07
	KEL2-10	0.06703	0.00129	1.17569	0.02249	0.12720	0.00149	0.03825	0.00065	839	21	789	10	772	9	759	13	2.20%	0.67
	KEL2-100	0.06661	0.00179	1.21647	0.03242	0.13242	0.00174	0.03923	0.00108	826	34	808	15	802	10	778	21	0.75%	0.68
	KEL2-11	0.05850	0.00134	0.70788	0.01608	0.08775	0.00106	0.02857	0.00053	549	29	543	10	542	6	569	10	0.18%	0.49
	KEL2-12	0.05915	0.00125	0.67911	0.01415	0.08325	0.00099	0.02609	0.00046	573	25	526	9	515	6	521	9	2.14%	0.59
	KEL2-14	0.06154	0.00175	0.90125	0.02314	0.10622	0.00128	0.03271	0.00050	658	62	652	12	651	7	650	10	0.15%	0.08
	KEL2-15	0.05982	0.00147	0.70525	0.01530	0.08550	0.00099	0.02641	0.00029	597	55	542	9	529	6	527	6	2.46%	0.11
	KEL2-16	0.05972	0.00133	0.74253	0.01632	0.09016	0.00109	-0.00085	0.04733	593	27	564	10	556	6	-17	17	1.44%	0.00
	KEL2-18	0.07021	0.00197	1.22024	0.03093	0.12605	0.00151	0.03823	0.00060	935	59	810	14	765	9	758	12	5.88%	0.11
	KEL2-19	0.07209	0.00337	1.49636	0.06879	0.15052	0.00226	0.04738	0.00148	988	69	929	28	904	13	936	29	2.77%	0.60
	KEL2-20	0.11848	0.00216	5.20670	0.09490	0.31867	0.00371	0.09293	0.00156	1933	17	1854	16	1783	18	1796	29	8.41%	0.72
	KEL2-21	0.06155	0.00164	0.87075	0.02277	0.10258	0.00130	0.03248	0.00065	659	35	636	12	630	8	646	13	0.95%	0.83
	KEL2-23	0.05893	0.00194	0.67701	0.02191	0.08331	0.00110	0.02591	0.00055	565	47	525	13	516	7	517	11	1.74%	0.90
	KEL2-24	0.05870	0.00124	0.69005	0.01445	0.08525	0.00102	0.02501	0.00060	556	26	533	9	527	6	499	12	1.14%	0.15
	KEL2-25	0.06291	0.00138	0.83813	0.01813	0.09661	0.00117	0.04039	0.00105	705	26	618	10	595	7	800	20	3.87%	0.13
	KEL2-26	0.05867	0.00157	0.66266	0.01590	0.08192	0.00098	0.02536	0.00029	555	60	516	10	508	6	506	6	1.57%	0.06
	KEL2-27	0.06586	0.00253	1.07243	0.04058	0.11808	0.00160	0.04081	0.00113	802	56	740	20	720	9	808	22	2.78%	0.44
	KEL2-29	0.07420	0.00970	1.74728	0.22502	0.17076	0.00476	0.06129	0.00552	1047	25	1026	83	1016	26	1202	15	3.05%	0.44
	KEL2-31	0.05837	0.00159	0.66302	0.01773	0.08237	0.00105	0.02570	0.00053	544	36	516	11	510	6	513	10	1.18%	0.76
	KEL2-32	0.05972	0.00120	0.75107	0.01502	0.09120	0.00108	0.02758	0.00051	593	24	569	9	563	6	550	10	1.07%	0.46
	KEL2-34	0.05923	0.00152	0.72595	0.01847	0.08887	0.00110	0.02857	0.00069	576	34	554	11	549	7	569	14	0.91%	0.25
	KEL2-36	0.06045	0.00122	0.81516	0.01639	0.09778	0.00116	0.03740	0.00133	620	24	605	9	601	7	742	26	0.67%	0.03
	KEL2-37	0.05818	0.00128	0.67860	0.01478	0.08458	0.00103	0.02763	0.00058	537	27	526	9	523	6	551	11	0.57%	0.26
	KEL2-40	0.06013	0.00143	0.78636	0.01842	0.09483	0.00117	0.02949	0.00078	608	30	589	10	584	7	587	15	0.86%	0.19
	KEL2-41	0.05972	0.00152	0.75104	0.01884	0.09119	0.00114	0.02856	0.00074	593	33	569	11	563	7	569	15	1.07%	0.27
	KEL2-42	0.05884	0.00153	0.66259	0.01697	0.08166	0.00103	0.02537	0.00058	561	34	516	10	506	6	506	11	1.98%	0.44
	KEL2-44	0.06482	0.00149	0.81420	0.01857	0.09108	0.00112	0.04010	0.00092	768	28	605	10	562	7	795	18	7.65%	0.22
	KEL2-45	0.06240	0.00136	0.90294	0.01943	0.10492	0.00128	0.03016	0.00077	688	26	653	10	643	7	601	15	1.56%	0.13
	KEL2-48	0.05809	0.00125	0.75935	0.01625	0.09478	0.00115	0.02835	0.00094	533	26	574	9	584	7	565	18	1.71%	0.06
	KEL2-49	0.05782	0.00204	0.65685	0.02283	0.08238	0.00112	0.02437	0.00061	523	52	513	14	510	7	487	12	0.59%	0.77
	KEL2-50	0.05732	0.00143	0.64117	0.01580	0.08111	0.00102	0.02508	0.00053	504	32	503	10	503	6	501	10	0.00%	0.91
	KEL2-53	0.06444	0.00389	1.17277	0.06982	0.13197	0.00211	0.03821	0.00160	756	99	788	33	799	12	758	31	1.38%	0.65
	KEL2-56	0.05835	0.00143	0.68817	0.01667	0.08552	0.00107	0.02573	0.00116	543	31	532	10	529	6	513	23	0.57%	0.07
	KEL2-58	0.06062	0.00130	0.74801	0.01593	0.08947	0.00108	0.03035	0.00071	626	26	567	9	552	6	604	14	2.72%	0.06
	KEL2-60	0.06382	0.00159	0.90788	0.02231	0.10315	0.00131	0.04868	0.00125	736	31	656	12	633	8	961	24	3.63%	0.18
	KEL2-61	0.07321	0.00214	1.54801	0.04440	0.15333	0.00206	0.04317	0.00107	1020	36	950	18	920	12	854	21	3.26%	0.77
	KEL2-63	0.05854	0.00155	0.67455	0.01767	0.08356	0.00107	0.02550	0.00066	550	35	523	11	517	6	509	13	1.16%	0.36
	KEL2-64	0.06789	0.00214	1.00751	0.03121	0.10762	0.00146	0.03401	0.00077	865	42	708	16	659	8	676	15	7.44%	2.03
	KEL2-65	0.05827	0.00151	0.70064	0.01798	0.08719	0.00112	0.02601	0.00072	540	34	539	11	539	7	519	14	0.00%	0.25
	KEL2-66	0.06360	0.00430	1.02263	0.06741	0.11661	0.00175	0.03577	0.00040	728	17	715	34	711	10	710	8	0.56%	0.87
	KEL2-67	0.06470	0.00314	1.11884	0.05355	0.12540	0.00185	0.04019	0.00106	765	76	762	26	762	11	796	21	0.00%	1.17
	KEL2-68	0.11501	0.00270	5.02507	0.11668	0.31683	0.00404	0.09006	0.00210	1880	24	1824	20	1774	20	1743	39	5.98%	0.60
	KEL2-69	0.05815	0.00153	0.69595	0.01804	0.08678	0.00111	0.02706	0.00075	535	35	536	11	536	7	540	15	0.00%	0.19
	KEL2-71	0.05973	0.00143	0.75107	0.01778	0.09118	0.00114	0.02672	0.00065	594	30	569	10	563	7	533	13	1.07%	0.23
	KEL2-73	0.06846	0.00161	1.21002	0.02819	0.12816	0.00160	0.04706	0.00110	883	28	805	13	777	9	929	21	3.60%	0.35
	KEL2-74	0.06679	0.00160	1.07860	0.02564	0.11709	0.00148	0.03793	0.00087	831	29	743	13	714	9	752	17	4.06%	1.11
	KEL2-78	0.05834	0.00149	0.68114	0.01722	0.08466	0.00109	0.02581	0.00067	543	33	527	10	524	6	515	13	0.57%	0.27
	KEL2-80	0.06335	0.00165	0.97770	0.02524	0.11192	0.00145	0.03658	0.00092	720	33	692	13	684	8	726	18	1.17%	0.48
	KEL2-83	0.06131	0.00150	0.79097	0.01927	0.09355	0.00119	0.02970	0.00076	650	31	592	11	576	7	592	15	2.78%	0.12
	KEL2-86	0.06042	0.00158	0.76896	0.01990	0.09228	0.00120	0.02722	0.00070	619	34	579	11	569	7	543	14	1.76%	0.70

(*continued on next page*)

Table 2 (*continued*)

River	Analysis (Sample No. and Spot No.)	CORRECTED RATIOS $^{207}Pb/^{206}Pb$	1σ	$^{207}Pb/^{235}U$	1σ	$^{206}Pb/^{238}U$	1σ	$^{208}Pb/^{232}Th$	1σ	CORRECTED AGES (Ma) $^{207}Pb/^{206}Pb$	1σ	$^{207}Pb/^{235}U$	1σ	$^{206}Pb/^{238}U$	1σ	$^{208}Pb/^{232}Th$	1σ	Degree of Discordance	Th/U
	KEL2-87	0.07202	0.00206	1.67358	0.04708	0.16849	0.00229	0.04865	0.00134	987	35	999	18	1004	13	960	26	1.69%	0.60
	KEL2-88	0.11480	0.00294	5.02351	0.12737	0.31731	0.00415	0.09146	0.00238	1877	27	1823	21	1777	20	1769	44	5.63%	0.64
	KEL2-89	0.07230	0.00220	1.48655	0.04459	0.14909	0.00205	0.04216	0.00117	994	39	925	18	896	12	835	23	3.24%	0.87
	KEL2-93	0.06485	0.07327	1.04954	1.18010	0.11735	0.01349	0.05502	0.01855	769	16	729	585	715	78	1083	35	1.96%	0.11
	KEL2-95	0.05835	0.00307	0.73259	0.03810	0.09104	0.00141	0.02344	0.00210	543	87	558	22	562	8	468	41	0.71%	0.84
	KEL2-96	0.11631	0.00370	4.95676	0.15447	0.30901	0.00462	0.07301	0.00715	1900	35	1812	26	1736	23	1424	15	9.45%	0.18
Kalu	**KLL1-001**	0.06823	0.00705	1.22496	0.12425	0.13022	0.00253	0.03963	0.00053	875	23	812	57	789	14	785	10	2.92%	0.49
	KLL1-002	0.06883	0.03564	1.36898	0.70542	0.14423	0.00808	0.05436	0.01463	894	21	876	302	869	46	1070	20	0.81%	0.55
	KLL1-005	0.07019	0.00584	1.56547	0.12867	0.16173	0.00306	0.04750	0.00201	934	23	957	51	966	17	938	39	0.93%	0.73
	KLL1-006	0.12418	0.00178	6.25013	0.09196	0.36497	0.00434	0.09549	0.00134	2017	12	2011	13	2006	20	1843	25	0.55%	0.63
	KLL1-008	0.06012	0.00092	0.76890	0.01201	0.09274	0.00109	0.02736	0.00054	608	16	579	7	572	6	546	11	1.22%	0.11
	KLL1-009	0.06469	0.00151	1.10719	0.02234	0.12413	0.00146	0.03800	0.00044	764	50	757	11	754	8	754	9	0.40%	0.22
	KLL1-010	0.07152	0.00143	1.57647	0.03150	0.15983	0.00200	0.04571	0.00068	972	21	961	12	956	11	903	13	0.52%	1.26
	KLL1-011	0.06818	0.00162	1.36036	0.03192	0.14467	0.00187	0.04298	0.00087	874	28	872	14	871	11	851	17	0.11%	0.56
	KLL1-012	0.05806	0.00095	0.69126	0.01148	0.08633	0.00103	0.02603	0.00046	532	18	534	7	534	6	519	9	0.00%	0.23
	KLL1-013	0.05869	0.00207	0.71044	0.02472	0.08778	0.00122	0.02650	0.00056	556	52	545	15	542	7	529	11	0.55%	0.71
	KLL1-014	0.05937	0.00111	0.78532	0.01476	0.09591	0.00116	0.04311	0.00130	581	21	589	8	590	7	853	25	0.17%	0.09
	KLL1-015	0.05778	0.00141	0.66332	0.01607	0.08325	0.00106	0.02416	0.00165	521	31	517	10	515	6	483	33	0.39%	0.07
	KLL1-016	0.05949	0.00150	0.82875	0.02084	0.10101	0.00127	0.02980	0.00112	585	33	613	12	620	7	594	22	1.13%	0.15
	KLL1-017	0.06105	0.00780	0.86758	0.10987	0.10304	0.00224	0.03083	0.00102	641	24	634	60	632	13	614	20	0.32%	1.54
	KLL1-018	0.07455	0.00300	1.73856	0.06885	0.16910	0.00254	0.05038	0.00143	1056	55	1023	26	1007	14	993	28	4.87%	0.60
	KLL1-019	0.06775	0.00443	1.35218	0.08742	0.14471	0.00240	0.04010	0.00137	861	10	869	38	871	14	795	27	0.23%	0.84
	KLL1-020	0.05658	0.00081	0.78040	0.01155	0.10001	0.00117	0.02599	0.00042	475	15	586	7	614	7	519	8	4.56%	0.10
	KLL1-021	0.06417	0.00103	1.13260	0.01852	0.12797	0.00152	0.04155	0.00068	747	17	769	9	776	9	823	13	0.90%	0.28
	KLL1-022	0.07143	0.00147	1.23135	0.02520	0.12500	0.00157	0.04723	0.00090	970	22	815	11	759	9	933	17	7.38%	0.37
	KLL1-025	0.06851	0.00107	1.27391	0.02029	0.13483	0.00160	0.03906	0.00053	884	16	834	9	815	9	774	10	2.33%	2.04
	KLL1-029	0.06042	0.00105	0.82449	0.01443	0.09895	0.00119	0.03203	0.00087	619	19	611	8	608	7	637	17	0.49%	0.09
	KLL1-031	0.05985	0.00272	0.79389	0.03566	0.09617	0.00140	0.02624	0.00075	598	72	593	20	592	8	524	15	0.17%	0.73
	KLL1-032	0.05873	0.00302	0.72968	0.03699	0.09008	0.00137	0.02565	0.00065	557	84	556	22	556	8	512	13	0.00%	0.89
	KLL1-034	0.07461	0.00165	1.39515	0.03066	0.13559	0.00173	0.03004	0.00048	1058	24	887	13	820	10	598	9	8.17%	1.75
	KLL1-035	0.06297	0.00266	0.87515	0.03650	0.10077	0.00145	0.03063	0.00089	707	64	638	20	619	8	610	17	3.07%	0.58
	KLL1-036	0.05733	0.00163	0.68071	0.01919	0.08609	0.00113	0.02508	0.00070	504	39	527	12	532	7	501	14	0.94%	0.28
	KLL1-037	0.06122	0.00145	0.77535	0.01584	0.09186	0.00110	0.02830	0.00032	647	52	583	9	567	6	564	6	2.82%	0.10
	KLL1-039	0.12593	0.00195	6.03954	0.09515	0.34774	0.00415	0.09461	0.00153	2042	13	1982	14	1924	20	1827	28	6.13%	0.37
	KLL1-040	0.06158	0.00122	0.61784	0.01215	0.07275	0.00090	0.01659	0.00024	660	22	488	8	453	5	333	5	7.73%	0.23
	KLL1-041	0.06474	0.00151	1.08459	0.02183	0.12150	0.00144	0.03720	0.00042	766	50	746	11	739	8	738	8	0.95%	0.19
	KLL1-042	0.05780	0.00096	0.71425	0.01201	0.08960	0.00107	0.02623	0.00065	522	18	547	7	553	6	523	13	1.08%	0.06
	KLL1-043	0.06939	0.00111	1.49321	0.02430	0.15602	0.00186	0.04164	0.00062	910	16	928	10	935	10	825	12	0.75%	1.45
	KLL1-046	0.05906	0.00293	0.73450	0.03602	0.09018	0.00132	0.02643	0.00055	569	81	559	21	557	8	527	11	0.36%	1.34
	KLL1-047	0.06652	0.00106	0.92068	0.01485	0.10035	0.00119	0.01082	0.00016	823	16	663	8	616	7	218	3	7.63%	2.82
	KLL1-048	0.07219	0.00380	1.41632	0.07157	0.14230	0.00213	0.04303	0.00053	991	11	896	30	858	12	852	10	4.43%	0.89
	KLL1-050	0.07328	0.00134	1.55881	0.02858	0.15424	0.00189	0.04538	0.00076	1022	19	954	11	925	11	897	15	3.14%	0.78
	KLL1-051	0.06019	0.00131	0.76228	0.01649	0.09182	0.00116	0.02607	0.00066	610	26	575	10	566	7	520	13	1.59%	0.26
	KLL1-052	0.06756	0.00212	1.24500	0.03864	0.13361	0.00179	0.03873	0.00079	855	42	821	17	808	10	768	15	1.61%	0.90
	KLL1-055	0.06008	0.00131	0.72814	0.01345	0.08790	0.00103	0.02714	0.00032	606	48	555	8	543	6	541	6	2.21%	0.10
	KLL1-056	0.06684	0.00327	1.32751	0.06228	0.14405	0.00200	0.04394	0.00050	833	10	858	27	868	11	869	10	1.15%	0.89
	KLL1-057	0.07530	0.00128	1.66533	0.02850	0.16035	0.00193	0.04860	0.00081	1077	17	995	11	959	11	959	16	3.75%	0.48
	KLL1-058	0.07472	0.00201	1.57780	0.04184	0.15312	0.00204	0.04734	0.00129	1061	32	962	16	918	11	935	25	4.79%	0.38
	KLL1-059	0.06025	0.00108	0.78285	0.01403	0.09421	0.00114	0.06830	0.00275	613	19	587	8	580	7	1335	52	1.21%	0.01
	KLL1-060	0.06518	0.00118	1.11623	0.02023	0.12418	0.00151	0.03736	0.00076	780	19	761	10	755	9	741	15	0.79%	0.18

(*continued on next page*)

Table 2 (*continued*)

River	Analysis (Sample No. and Spot No.)	CORRECTED RATIOS $^{207}Pb/^{206}Pb$	1σ	$^{207}Pb/^{235}U$	1σ	$^{206}Pb/^{238}U$	1σ	$^{208}Pb/^{232}Th$	1σ	CORRECTED AGES (Ma) $^{207}Pb/^{206}Pb$	1σ	$^{207}Pb/^{235}U$	1σ	$^{206}Pb/^{238}U$	1σ	$^{208}Pb/^{232}Th$	1σ	Degree of Discordance	Th/U
	KLL1-061	0.06707	0.00125	1.07108	0.02000	0.11579	0.00142	0.04591	0.00079	840	20	739	10	706	8	907	15	4.67%	0.72
	KLL1-063	0.06656	0.00150	1.27849	0.02843	0.13927	0.00177	0.04079	0.00085	824	26	836	13	841	10	808	17	0.59%	0.47
	KLL1-064	0.06417	0.00122	0.94138	0.01780	0.10638	0.00131	0.02704	0.00051	747	21	674	9	652	8	539	10	3.37%	0.44
	KLL1-065	0.06537	0.00203	1.11729	0.03405	0.12394	0.00171	0.03947	0.00073	786	41	762	16	753	10	782	14	1.20%	2.06
	KLL1-066	0.05881	0.00169	0.67844	0.01924	0.08365	0.00109	0.02541	0.00077	560	39	526	12	518	6	507	15	1.54%	0.27
	KLL1-067	0.07431	0.00130	1.59487	0.02805	0.15562	0.00188	0.03200	0.00055	1050	18	968	11	932	10	637	11	3.86%	1.18
	KLL1-068	0.06542	0.00183	0.88436	0.02437	0.09802	0.00131	0.03159	0.00062	788	36	643	13	603	8	629	12	6.63%	1.14
	KLL1-069	0.06284	0.00110	0.86265	0.01519	0.09953	0.00120	0.03901	0.00070	703	19	632	8	612	7	773	14	3.27%	0.17
	KLL1-070	0.07175	0.00129	1.63176	0.02932	0.16490	0.00201	0.04620	0.00082	979	18	983	11	984	11	913	16	0.10%	0.59
	KLL1-071	0.05883	0.00289	0.70477	0.03412	0.08686	0.00129	0.02658	0.00068	561	80	542	20	537	8	530	13	0.93%	0.88
	KLL1-072	0.07271	0.00243	1.67641	0.05512	0.16718	0.00236	0.05090	0.00132	1006	44	1000	21	997	13	1003	25	0.30%	0.61
	KLL1-073	0.10421	0.00292	4.03446	0.10067	0.28077	0.00356	0.08164	0.00097	1701	53	1641	20	1595	18	1586	18	6.65%	0.48
	KLL1-074	0.06989	0.00135	1.23653	0.02372	0.12829	0.00159	0.02248	0.00043	925	20	817	11	778	9	449	9	5.01%	0.81
	KLL1-076	0.05991	0.00124	0.82630	0.01692	0.10001	0.00125	0.02699	0.00095	600	24	612	9	614	7	538	19	0.33%	0.11
	KLL1-078	0.05891	0.00149	0.74904	0.01865	0.09219	0.00119	0.03543	0.00219	564	32	568	11	568	7	704	43	0.00%	0.05
	KLL1-079	0.05974	0.00109	0.76404	0.01395	0.09274	0.00113	0.02750	0.00052	594	20	576	8	572	7	548	10	0.70%	0.20
	KLL1-080	0.06258	0.00122	0.79886	0.01550	0.09256	0.00114	0.03097	0.00168	694	22	596	9	571	7	616	33	4.38%	0.02
	KLL1-081	0.07156	0.00244	1.39529	0.04655	0.14139	0.00206	0.04208	0.00102	973	44	887	20	853	12	833	20	3.99%	0.95
	KLL1-082	0.06482	0.00132	1.12980	0.02277	0.12639	0.00158	0.03827	0.00074	768	22	768	11	767	9	759	14	0.13%	0.79
	KLL1-083	0.07822	0.00202	1.99098	0.05039	0.18458	0.00248	0.05525	0.00120	1152	29	1112	17	1092	13	1087	23	5.49%	0.85
	KLL1-084	0.06286	0.00170	0.78330	0.01884	0.09038	0.00113	0.02776	0.00061	703	59	587	11	558	7	553	12	5.20%	0.03
	KLL1-085	0.06537	0.00154	1.13165	0.02626	0.12554	0.00162	0.03619	0.00069	786	28	769	13	762	9	719	13	0.92%	3.92
	KLL1-086	0.07329	0.00170	1.56666	0.03573	0.15500	0.00201	0.04357	0.00098	1022	26	957	14	929	11	862	19	3.01%	0.56
	KLL1-087	0.07376	0.00170	1.53243	0.03479	0.15066	0.00194	0.04609	0.00099	1035	26	943	14	905	11	911	19	4.20%	0.67
	KLL1-088	0.07004	0.00143	1.43732	0.02897	0.14881	0.00186	0.04644	0.00096	930	22	905	12	894	10	918	19	1.23%	0.40
	KLL1-091	0.06509	0.00181	1.09585	0.03000	0.12209	0.00162	0.03755	0.00079	777	35	751	15	743	9	745	15	1.08%	1.23
	KLL1-092	0.06815	0.00430	1.20240	0.07485	0.12794	0.00215	0.03806	0.00152	873	11	802	35	776	12	755	30	3.35%	0.70
	KLL1-093	0.07345	0.00321	1.52341	0.06544	0.15041	0.00229	0.04767	0.00155	1026	62	940	26	903	13	941	30	4.10%	0.58
	KLL1-094	0.05804	0.00157	0.70134	0.01862	0.08763	0.00116	0.02691	0.00067	531	35	540	11	542	7	537	13	0.37%	0.44
	KLL1-095	0.06732	0.00278	1.07081	0.04333	0.11536	0.00176	0.03639	0.00083	848	59	739	21	704	10	722	16	4.97%	2.03
	KLL1-096	0.07540	0.00179	1.36578	0.03181	0.13136	0.00170	0.02535	0.00056	1079	27	874	14	796	10	506	11	9.80%	0.97
	KLL1-097	0.07848	0.00183	1.76279	0.04046	0.16289	0.00212	0.04887	0.00107	1159	26	1032	15	973	12	964	21	6.06%	0.79
	KLL1-098	0.06760	0.00187	1.25366	0.03392	0.13449	0.00181	0.03974	0.00093	856	34	825	15	813	10	788	18	1.48%	0.88
	KLL1-099	0.05974	0.00167	0.73499	0.02016	0.08922	0.00118	0.02259	0.00112	594	37	559	12	551	7	452	22	1.45%	0.12
	KLL1-100	0.05841	0.00141	0.70920	0.01685	0.08805	0.00114	0.02732	0.00064	545	30	544	10	544	7	545	13	0.00%	0.43
	KLL1-101	0.06781	0.00178	1.17362	0.03013	0.12551	0.00168	0.03887	0.00088	863	31	788	14	762	10	771	17	3.41%	0.98
	KLL1-103	0.07220	0.00257	1.33873	0.04431	0.13448	0.00176	0.04067	0.00047	992	74	863	19	813	10	806	9	6.15%	0.50
	KLL1-104	0.06688	0.00158	1.29719	0.03000	0.14066	0.00183	0.04358	0.00094	834	27	844	13	848	10	862	18	0.47%	1.30
	KLL1-105	0.05957	0.00162	0.72329	0.01933	0.08805	0.00117	0.02599	0.00072	588	35	553	11	544	7	519	14	1.65%	0.29
	KLL1-106	0.07033	0.00249	1.15067	0.03986	0.11865	0.00173	0.07322	0.00189	938	47	778	19	723	10	1428	36	7.61%	0.51
	KLL1-107	0.07352	0.00169	1.25355	0.02825	0.12365	0.00160	0.03315	0.00080	1028	25	825	13	752	9	659	16	9.71%	0.40
	KLL1-108	0.07228	0.00156	1.43886	0.03054	0.14437	0.00183	0.04360	0.00094	994	23	905	13	869	10	863	18	4.14%	0.87
	KLL1-109	0.07332	0.00333	1.57909	0.06803	0.15620	0.00225	0.04715	0.00058	1023	94	962	27	936	13	931	11	2.78%	0.53
	KLL1-110	0.05948	0.00139	0.73030	0.01673	0.08904	0.00115	0.02744	0.00065	585	28	557	10	550	7	547	13	1.27%	0.31
	KLL1-111	0.06464	0.00243	1.08013	0.03979	0.12119	0.00174	0.05033	0.00365	763	53	744	19	737	10	993	70	0.95%	0.11
	KLL1-112	0.06707	0.00196	1.24050	0.03542	0.13415	0.00184	0.04102	0.00130	840	37	819	16	811	10	813	25	0.99%	0.26
	KLL1-114	0.07060	0.00256	1.36490	0.04856	0.14021	0.00202	0.04350	0.00118	946	49	874	21	846	11	861	23	3.31%	0.67
	KLL1-116	0.06824	0.00339	1.28333	0.06088	0.13639	0.00199	0.04150	0.00050	876	15	838	27	824	11	822	10	1.70%	0.54
	KLL1-117	0.06539	0.00164	1.02668	0.02512	0.11387	0.00150	0.03837	0.00092	787	30	717	13	695	9	761	18	3.17%	0.61
	KLL1-118	0.07095	0.00162	1.35655	0.03038	0.13867	0.00179	0.04253	0.00098	956	25	870	13	837	10	842	19	3.94%	0.56

(*continued on next page*)

Table 2 (*continued*)

River	Analysis (Sample No. and Spot No.)	CORRECTED RATIOS $^{207}Pb/^{206}Pb$	1σ	$^{207}Pb/^{235}U$	1σ	$^{206}Pb/^{238}U$	1σ	$^{208}Pb/^{232}Th$	1σ	CORRECTED AGES (Ma) $^{207}Pb/^{206}Pb$	1σ	$^{207}Pb/^{235}U$	1σ	$^{206}Pb/^{238}U$	1σ	$^{208}Pb/^{232}Th$	1σ	Degree of Discordance	Th/U
	KLL1-119	0.06583	0.00151	0.99386	0.02236	0.10950	0.00141	0.03372	0.00080	801	26	701	11	670	8	670	16	4.63%	0.32
	KLL1-120	0.07281	0.00163	1.69558	0.03732	0.16889	0.00216	0.04934	0.00113	1009	25	1007	14	1006	12	973	22	0.30%	0.59
Walawe	**WAL1-03**	0.11179	0.00292	5.10478	0.13165	0.33107	0.00444	0.07261	0.00198	1829	28	1837	22	1844	22	1417	37	0.81%	0.60
	WAL1-05	0.06879	0.00161	1.35190	0.03159	0.14249	0.00178	0.03446	0.00178	892	28	868	14	859	10	685	35	1.05%	0.04
	WAL1-06	0.06502	0.00188	0.81670	0.02337	0.09107	0.00118	0.02607	0.00065	775	38	606	13	562	7	520	13	7.83%	0.49
	WAL1-11	0.06316	0.00139	0.90209	0.01991	0.10355	0.00126	0.03281	0.00081	714	27	653	11	635	7	653	16	2.83%	0.07
	WAL1-13	0.07588	0.00181	1.53027	0.03623	0.14622	0.00185	0.04425	0.00108	1092	28	943	15	880	10	875	21	7.16%	0.31
	WAL1-15	0.06278	0.00159	0.80395	0.02015	0.09285	0.00117	0.02581	0.00057	701	32	599	11	572	7	515	11	4.72%	0.79
	WAL1-16	0.06301	0.00154	0.84642	0.01814	0.09743	0.00116	0.02992	0.00034	709	53	623	10	599	7	596	7	4.01%	0.02
	WAL1-18	0.06035	0.00136	0.79216	0.01778	0.09517	0.00117	0.02746	0.00067	616	28	592	10	586	7	548	13	1.02%	0.08
	WAL1-25	0.06103	0.00151	0.74486	0.01824	0.08850	0.00112	0.04183	0.00126	640	31	565	11	547	7	828	24	3.29%	0.07
	WAL1-26	0.06981	0.00166	1.38172	0.03261	0.14350	0.00179	0.04854	0.00114	923	28	881	14	864	10	958	22	1.97%	0.30
	WAL1-32	0.06041	0.00182	0.62989	0.01738	0.07562	0.00092	0.02333	0.00028	618	67	496	11	470	6	466	6	5.53%	0.12
	WAL1-34	0.06003	0.00144	0.81645	0.01955	0.09861	0.00123	0.06261	0.00342	605	31	606	11	606	7	1227	65	0.00%	0.01
	WAL1-36	0.06542	0.00207	1.02994	0.02997	0.11418	0.00143	0.03491	0.00063	788	68	719	15	697	8	694	12	3.16%	0.07
	WAL1-37	0.06145	0.00151	0.76330	0.01862	0.09007	0.00113	0.02860	0.00071	655	31	576	11	556	7	570	14	3.60%	0.21
	WAL1-40	0.06014	0.00147	0.75570	0.01837	0.09110	0.00114	0.02882	0.00074	609	31	572	11	562	7	574	15	1.78%	0.09
	WAL1-42	0.11673	0.00288	5.02392	0.12305	0.31207	0.00393	0.08924	0.00220	1907	26	1823	21	1751	19	1728	41	8.91%	0.49
	WAL1-44	0.13581	0.00340	6.85916	0.17041	0.36620	0.00467	0.10018	0.00252	2174	26	2093	22	2011	22	1930	46	8.11%	0.70
	WAL1-46	0.06616	0.00190	0.83392	0.02364	0.09139	0.00121	0.02864	0.00078	811	37	616	13	564	7	571	15	9.22%	0.65
	WAL1-47	0.07078	0.00202	1.48601	0.04187	0.15224	0.00203	0.04551	0.00127	951	36	925	17	914	11	900	25	1.20%	0.51
	WAL1-52	0.11572	0.00310	5.31927	0.14080	0.33329	0.00435	0.09377	0.00255	1891	29	1872	23	1854	21	1812	47	2.00%	0.64
	WAL1-53	0.06063	0.00163	0.81844	0.02173	0.09788	0.00126	0.02907	0.00080	626	35	607	12	602	7	579	16	0.83%	0.31
	WAL1-55	0.06162	0.00169	0.78733	0.02133	0.09265	0.00120	0.02842	0.00090	661	36	590	12	571	7	566	18	3.33%	0.09
	WAL1-59	0.11617	0.00319	5.33326	0.14469	0.33288	0.00436	0.09486	0.00268	1898	30	1874	23	1852	21	1832	49	2.48%	0.54
	WAL1-60	0.05959	0.00174	0.73638	0.02118	0.08960	0.00119	0.02724	0.00078	589	39	560	12	553	7	543	15	1.27%	0.85
	WAL1-61	0.06190	0.00181	0.84031	0.02423	0.09843	0.00131	0.02980	0.00092	671	39	619	13	605	8	594	18	2.31%	0.25
	WAL1-64	0.21786	0.00657	18.65612	0.55322	0.62094	0.00908	0.17149	0.00571	2965	29	3024	29	3114	36	3199	99	4.78%	0.74
	WAL1-70	0.06105	0.00190	0.79053	0.02421	0.09389	0.00128	0.03959	0.00381	641	42	591	14	579	8	785	74	2.07%	0.02
	WAL1-74	0.06123	0.00201	0.84113	0.02535	0.09964	0.00131	0.03070	0.00042	647	72	620	14	612	8	611	8	1.31%	0.03
	WAL1-75	0.06274	0.00218	0.87859	0.03000	0.10153	0.00144	0.03385	0.01304	699	49	640	16	623	8	673	25	2.73%	0.01
	WAL1-77	0.06434	0.00244	0.88759	0.03307	0.10003	0.00147	0.02991	0.00111	753	54	645	18	615	9	596	22	4.88%	0.49
	WAL1-81	0.06130	0.00195	0.77830	0.02432	0.09207	0.00126	0.02926	0.00110	650	44	585	14	568	7	583	22	2.99%	0.03
	WAL1-82	0.06108	0.00272	0.74313	0.03247	0.08823	0.00137	0.02815	0.00106	642	67	564	19	545	8	561	21	3.49%	0.79
	WAL1-83	0.06014	0.00193	0.79749	0.02512	0.09616	0.00132	0.03038	0.00118	609	44	595	14	592	8	605	23	0.51%	0.02
	WAL1-88	0.06271	0.00216	0.87740	0.02780	0.10147	0.00139	0.03118	0.00056	699	75	640	15	623	8	621	11	2.73%	0.01
	WAL1-91	0.06097	0.00209	0.77113	0.02589	0.09171	0.00130	0.02983	0.00110	638	48	580	15	566	8	594	22	2.47%	0.22
	WAL1-92	0.06502	0.00270	0.97708	0.03826	0.10899	0.00153	0.03335	0.00063	775	90	692	20	667	9	663	12	3.75%	0.07
	WAL1-93	0.14166	0.00495	7.55088	0.25836	0.38652	0.00567	0.11637	0.00440	2248	39	2179	31	2107	26	2225	80	6.69%	0.60
	WAL1-95	0.07161	0.00255	1.12697	0.03930	0.11412	0.00165	0.05033	0.00193	975	47	766	19	697	10	993	37	9.90%	0.25
Maduru Oya	**MDL2-01**	0.11537	0.00097	5.24963	0.04419	0.32994	0.00372	0.07951	0.00104	1886	10	1861	7	1838	18	1546	19	2.61%	0.14
	MDL2-02	0.06557	0.00063	1.14710	0.01099	0.12685	0.00144	0.03649	0.00035	793	11	776	5	770	8	724	7	0.78%	0.88
	MDL2-03	0.05820	0.00095	0.69966	0.01116	0.08718	0.00104	0.02588	0.00036	537	16	539	7	539	6	516	7	0.00%	0.57
	MDL2-04	0.06539	0.00219	1.09390	0.03597	0.12130	0.00160	0.03928	0.00098	787	47	750	17	738	9	779	19	1.63%	0.37
	MDL2-05	0.06115	0.00057	0.77143	0.00713	0.09148	0.00103	0.02414	0.00027	645	11	581	4	564	6	482	5	3.01%	0.27
	MDL2-06	0.11100	0.00094	4.50754	0.03822	0.29446	0.00332	0.08104	0.00081	1816	10	1732	7	1664	17	1575	15	9.13%	0.43
	MDL2-07	0.06329	0.00063	1.05117	0.01048	0.12043	0.00136	0.03289	0.00051	718	11	729	5	733	8	654	10	0.55%	0.08
	MDL2-08	0.06575	0.00084	1.18744	0.01480	0.13097	0.00152	0.03932	0.00041	798	12	795	7	793	9	780	8	0.25%	1.01
	MDL2-09	0.05820	0.00075	0.74148	0.00938	0.09239	0.00107	0.02611	0.00038	537	12	563	5	570	6	521	7	1.23%	0.33

(*continued on next page*)

Table 2 (*continued*)

River	Analysis (Sample No. and Spot No.)	CORRECTED RATIOS $^{207}Pb/^{206}Pb$	1σ	$^{207}Pb/^{235}U$	1σ	$^{206}Pb/^{238}U$	1σ	$^{208}Pb/^{232}Th$	1σ	CORRECTED AGES (Ma) $^{207}Pb/^{206}Pb$	1σ	$^{207}Pb/^{235}U$	1σ	$^{206}Pb/^{238}U$	1σ	$^{208}Pb/^{232}Th$	1σ	Degree of Discordance	Th/U
	MDL2-10	0.05816	0.00066	0.70586	0.00788	0.08800	0.00101	0.02677	0.00029	536	11	542	5	544	6	534	6	0.37%	0.59
	MDL2-100	0.06460	0.00950	0.95827	0.13946	0.10756	0.00277	0.05241	0.00574	761	45	682	72	659	16	1032	23	3.49%	0.25
	MDL2-11	0.05898	0.00060	0.78240	0.00783	0.09620	0.00109	0.02633	0.00039	566	11	587	4	592	6	525	8	0.84%	0.13
	MDL2-12	0.06901	0.00124	0.99223	0.01387	0.10429	0.00118	0.03170	0.00041	899	38	700	7	639	7	631	8	9.55%	0.14
	MDL2-13	0.06195	0.00055	0.86182	0.00771	0.10089	0.00114	0.04705	0.00049	672	11	631	4	620	7	929	9	1.77%	0.16
	MDL2-15	0.06473	0.00149	1.07623	0.02401	0.12057	0.00155	0.03642	0.00052	766	26	742	12	734	9	723	10	1.09%	1.16
	MDL2-16	0.05978	0.00059	0.78215	0.00773	0.09487	0.00108	0.02696	0.00039	596	11	587	4	584	6	538	8	0.51%	0.12
	MDL2-18	0.06438	0.00118	0.94069	0.01341	0.10598	0.00122	0.03246	0.00039	754	40	673	7	649	7	646	8	3.70%	0.08
	MDL2-19	0.07136	0.00111	1.57543	0.02384	0.16009	0.00194	0.04821	0.00067	968	14	961	9	957	11	952	13	0.42%	0.65
	MDL2-20	0.06056	0.00055	0.62102	0.00562	0.07436	0.00084	0.01414	0.00023	624	11	490	4	462	5	284	5	6.06%	0.06
	MDL2-21	0.05955	0.00088	0.77639	0.01122	0.09454	0.00111	0.02778	0.00053	587	14	583	6	582	7	554	10	0.17%	0.17
	MDL2-22	0.05819	0.00125	0.70276	0.01478	0.08758	0.00108	0.02611	0.00061	537	25	540	9	541	6	521	12	0.18%	0.26
	MDL2-23	0.07367	0.00132	1.27809	0.01749	0.12583	0.00145	0.03797	0.00055	1032	37	836	8	764	8	753	11	9.42%	0.08
	MDL2-25	0.05715	0.00067	0.69728	0.00800	0.08848	0.00102	0.02510	0.00038	497	12	537	5	547	6	501	7	1.83%	0.20
	MDL2-26	0.05828	0.00129	0.72970	0.01376	0.09081	0.00106	0.02814	0.00032	540	50	556	8	560	6	561	6	0.71%	0.12
	MDL2-27	0.06538	0.00095	1.14256	0.01631	0.12672	0.00150	0.03932	0.00045	787	14	774	8	769	9	780	9	0.65%	1.18
	MDL2-28	0.05924	0.00076	0.76358	0.00965	0.09347	0.00109	0.02780	0.00039	576	12	576	6	576	6	554	8	0.00%	0.30
	MDL2-29	0.06797	0.00080	1.34196	0.01546	0.14317	0.00166	0.04119	0.00049	868	11	864	7	863	9	816	10	0.12%	0.54
	MDL2-31	0.06304	0.00316	1.00447	0.04962	0.11554	0.00173	0.03646	0.00067	710	23	706	25	705	10	724	13	0.14%	1.50
	MDL2-32	0.07562	0.00183	1.41377	0.02950	0.13560	0.00167	0.04079	0.00064	1085	50	895	12	820	10	808	12	9.15%	0.10
	MDL2-33	0.05947	0.00066	0.73124	0.00800	0.08917	0.00103	0.02431	0.00037	584	11	557	5	551	6	485	7	1.09%	0.14
	MDL2-34	0.05995	0.00066	0.77005	0.00839	0.09314	0.00107	0.02326	0.00035	602	11	580	5	574	6	465	7	1.05%	0.15
	MDL2-35	0.05910	0.00061	0.78171	0.00800	0.09592	0.00110	0.02745	0.00037	571	11	586	5	590	6	547	7	0.68%	0.13
	MDL2-36	0.05855	0.00091	0.72556	0.01105	0.08987	0.00107	0.02753	0.00056	550	15	554	7	555	6	549	11	0.18%	0.15
	MDL2-37	0.05890	0.00064	0.80078	0.00863	0.09860	0.00114	0.02898	0.00041	563	11	597	5	606	7	577	8	1.49%	0.15
	MDL2-38	0.05919	0.00130	0.73189	0.01566	0.08967	0.00111	0.02678	0.00046	574	26	558	9	554	7	534	9	0.72%	0.64
	MDL2-39	0.06069	0.00102	0.80594	0.01318	0.09630	0.00117	0.02920	0.00062	628	17	600	7	593	7	582	12	1.18%	0.19
	MDL2-41	0.05958	0.00090	0.77725	0.01152	0.09460	0.00113	0.02705	0.00042	588	15	584	7	583	7	539	8	0.17%	0.36
	MDL2-42	0.05873	0.00120	0.73216	0.01462	0.09040	0.00111	0.02778	0.00052	557	23	558	9	558	7	554	10	0.00%	0.39
	MDL2-45	0.06003	0.00104	0.77911	0.01318	0.09412	0.00114	0.02856	0.00040	605	18	585	8	580	7	569	8	0.86%	0.65
	MDL2-46	0.06002	0.00114	0.75980	0.01398	0.09180	0.00114	0.02796	0.00046	604	20	574	8	566	7	557	9	1.41%	0.57
	MDL2-47	0.05832	0.00343	0.67216	0.03908	0.08357	0.00125	0.02595	0.00046	542	10	522	24	517	7	518	9	0.97%	1.76
	MDL2-49	0.05854	0.00108	0.72367	0.01311	0.08964	0.00109	0.02670	0.00045	550	20	553	8	553	6	533	9	0.00%	0.44
	MDL2-51	0.05912	0.00082	0.76719	0.01046	0.09410	0.00111	0.02691	0.00035	572	13	578	6	580	7	537	7	0.34%	0.76
	MDL2-52	0.10962	0.00150	4.62465	0.06159	0.30594	0.00375	0.08747	0.00136	1793	11	1754	11	1721	19	1695	25	4.18%	0.55
	MDL2-53	0.06544	0.00146	0.98753	0.02149	0.10944	0.00138	0.03673	0.00050	789	25	697	11	669	8	729	10	4.19%	1.52
	MDL2-54	0.11483	0.00173	4.95146	0.07223	0.31269	0.00394	0.09362	0.00167	1877	12	1811	12	1754	19	1809	31	7.01%	0.46
	MDL2-57	0.05900	0.00075	0.75248	0.00947	0.09249	0.00109	0.02428	0.00074	567	12	570	5	570	6	485	15	0.00%	0.05
	MDL2-58	0.17877	0.00446	12.30161	0.25669	0.49909	0.00681	0.13758	0.00182	2641	42	2628	20	2610	29	2605	32	1.19%	0.98
	MDL2-59	0.06048	0.00091	0.79952	0.01171	0.09586	0.00116	0.00838	0.00029	621	14	597	7	590	7	169	6	1.19%	0.16
	MDL2-60	0.06230	0.00269	0.90892	0.03868	0.10580	0.00150	0.03860	0.00127	684	67	656	21	648	9	766	25	1.23%	0.32
	MDL2-61	0.06606	0.00215	1.17252	0.03712	0.12872	0.00184	0.03922	0.00079	808	42	788	17	781	11	778	15	0.90%	0.86
	MDL2-62	0.06060	0.00082	0.82343	0.01098	0.09854	0.00117	0.02819	0.00044	625	13	610	6	606	7	562	9	0.66%	0.28
	MDL2-64	0.05816	0.00132	0.71147	0.01583	0.08872	0.00112	0.02700	0.00046	536	27	546	9	548	7	538	9	0.36%	0.72
	MDL2-65	0.05760	0.00101	0.67761	0.01166	0.08530	0.00104	0.02509	0.00058	515	18	525	7	528	6	501	11	0.57%	0.17
	MDL2-67	0.05912	0.00130	0.71543	0.01544	0.08776	0.00110	0.02464	0.00065	572	26	548	9	542	7	492	13	1.11%	0.26
	MDL2-68	0.06221	0.00095	0.80096	0.01195	0.09337	0.00113	0.02758	0.00065	681	15	597	7	575	7	550	13	3.83%	0.12
	MDL2-69	0.06579	0.00201	1.19774	0.03567	0.13201	0.00180	0.04060	0.00065	800	40	800	16	799	10	804	13	0.13%	1.79
	MDL2-70	0.06252	0.00114	0.97433	0.01733	0.11302	0.00141	0.02207	0.00082	692	19	691	9	690	8	441	16	0.14%	0.13
	MDL2-71	0.06059	0.00107	0.76531	0.01319	0.09159	0.00113	0.01539	0.00094	625	18	577	8	565	7	309	19	2.12%	0.08

(*continued on next page*)

Table 2 (*continued*)

River	Analysis (Sample No. and Spot No.)	CORRECTED RATIOS								CORRECTED AGES (Ma)									
		$^{207}Pb/^{206}Pb$	1σ	$^{207}Pb/^{235}U$	1σ	$^{206}Pb/^{238}U$	1σ	$^{208}Pb/^{232}Th$	1σ	$^{207}Pb/^{206}Pb$	1σ	$^{207}Pb/^{235}U$	1σ	$^{206}Pb/^{238}U$	1σ	$^{208}Pb/^{232}Th$	1σ	Degree of Discordance	Th/U
	MDL2-73	0.05785	0.00163	0.67324	0.01861	0.08438	0.00111	0.02512	0.00059	524	38	523	11	522	7	501	12	0.19%	0.43
	MDL2-74	0.06055	0.00107	0.84326	0.01462	0.10098	0.00125	0.03237	0.00056	623	18	621	8	620	7	644	11	0.16%	0.40
	MDL2-75	0.11313	0.00171	5.20192	0.07656	0.33343	0.00415	0.09453	0.00159	1850	12	1853	13	1855	20	1826	29	0.27%	0.55
	MDL2-77	0.05885	0.00167	0.70961	0.01969	0.08743	0.00115	0.00791	0.00118	562	38	545	12	540	7	159	24	0.93%	0.13
	MDL2-78	0.05939	0.00222	0.69399	0.02430	0.08475	0.00110	0.02620	0.00030	582	83	535	15	524	7	523	6	2.10%	0.50
	MDL2-79	0.07060	0.00132	1.56689	0.02867	0.16094	0.00203	0.04650	0.00074	946	19	957	11	962	11	919	14	0.52%	0.94
	MDL2-80	0.05777	0.00128	0.67073	0.01456	0.08419	0.00106	0.02614	0.00044	521	26	521	9	521	6	522	9	0.00%	0.73
	MDL2-81	0.10390	0.00294	4.20373	0.11572	0.29337	0.00423	0.06544	0.00174	1695	30	1675	23	1658	21	1281	33	2.23%	0.69
	MDL2-82	0.11850	0.00169	5.62815	0.07865	0.34439	0.00424	0.09150	0.00191	1934	11	1920	12	1908	20	1770	35	1.36%	0.18
	MDL2-83	0.05924	0.00087	0.77010	0.01109	0.09427	0.00114	0.02521	0.00041	576	14	580	6	581	7	503	8	0.17%	0.34
	MDL2-85	0.06008	0.00084	0.82813	0.01137	0.09995	0.00120	0.02990	0.00057	606	13	613	6	614	7	595	11	0.16%	0.09
	MDL2-89	0.06980	0.00107	1.05305	0.01589	0.10940	0.00134	0.02876	0.00061	922	14	730	8	669	8	573	12	9.12%	0.16
	MDL2-90	0.05980	0.00116	0.72794	0.01125	0.08829	0.00104	0.02728	0.00044	596	43	555	7	545	6	544	9	1.83%	0.05
	MDL2-91	0.06753	0.00097	1.15238	0.01638	0.12375	0.00150	0.03741	0.00057	854	13	778	8	752	9	742	11	3.46%	0.69
	MDL2-93	0.07013	0.00115	1.40692	0.02255	0.14548	0.00181	0.04444	0.00074	932	15	892	10	876	10	879	14	1.83%	0.59
	MDL2-94	0.11466	0.00166	5.33717	0.07611	0.33754	0.00415	0.09457	0.00153	1875	12	1875	12	1875	20	1826	28	0.00%	0.58
	MDL2-98	0.06233	0.00629	0.93634	0.09312	0.10893	0.00237	0.03722	0.00171	685	56	671	49	667	14	739	33	0.60%	0.63
	MDL2-99	0.05969	0.01168	0.76986	0.14918	0.09352	0.00291	0.02648	0.00104	592	56	580	86	576	17	528	20	0.69%	2.31
Maha Oya	**MOL1-02**	0.05980	0.00140	0.73551	0.01487	0.08921	0.00105	0.02756	0.00033	596	52	560	9	551	6	550	7	1.63%	0.11
	MOL1-03	0.07685	0.00327	1.51728	0.06135	0.14320	0.00191	0.04300	0.00051	1117	87	937	25	863	11	851	10	8.57%	0.65
	MOL1-04	0.06525	0.00151	1.01275	0.02016	0.11256	0.00133	0.03443	0.00040	783	50	710	10	688	8	684	8	3.20%	0.13
	MOL1-05	0.07632	0.00323	1.72166	0.06909	0.16360	0.00219	0.04917	0.00057	1104	87	1017	26	977	12	970	11	4.09%	0.71
	MOL1-06	0.06894	0.00116	1.26936	0.02158	0.13353	0.00159	0.02192	0.00036	897	17	832	10	808	9	438	7	2.97%	0.24
	MOL1-07	0.05797	0.00105	0.73246	0.01340	0.09162	0.00111	0.02604	0.00050	529	20	558	8	565	7	520	10	1.24%	0.20
	MOL1-08	0.05935	0.00108	0.74883	0.01370	0.09149	0.00110	0.02441	0.00055	580	20	568	8	564	6	487	11	0.71%	0.10
	MOL1-09	0.06377	0.00136	0.98853	0.02102	0.11241	0.00141	0.03385	0.00059	734	25	698	11	687	8	673	12	1.60%	1.23
	MOL1-10	0.06689	0.00115	1.18975	0.02069	0.12898	0.00154	0.03812	0.00062	834	18	796	10	782	9	756	12	1.79%	0.84
	MOL1-11	0.06560	0.00115	1.14131	0.02023	0.12616	0.00151	0.03261	0.00055	794	19	773	10	766	9	649	11	0.91%	0.55
	MOL1-12	0.06159	0.00107	0.84315	0.01485	0.09927	0.00119	0.02117	0.00042	660	19	621	8	610	7	423	8	1.80%	0.10
	MOL1-14	0.06970	0.00227	1.50641	0.04520	0.15675	0.00196	0.04759	0.00054	920	68	933	18	939	11	940	10	0.64%	0.46
	MOL1-15	0.05911	0.00125	0.75570	0.01338	0.09272	0.00108	0.02869	0.00034	571	47	572	8	572	6	572	7	0.00%	0.04
	MOL1-16	0.07215	0.00130	1.61594	0.02935	0.16242	0.00196	0.04763	0.00080	990	19	976	11	970	11	940	15	0.62%	1.09
	MOL1-17	0.07093	0.00127	1.38304	0.02493	0.14141	0.00170	0.04424	0.00076	955	19	882	11	853	10	875	15	3.40%	0.52
	MOL1-18	0.07178	0.00134	1.71783	0.03215	0.17355	0.00212	0.05540	0.00098	980	20	1015	12	1032	12	1090	19	5.04%	0.57
	MOL1-19	0.07726	0.00149	1.68768	0.03253	0.15841	0.00195	0.04839	0.00090	1128	20	1004	12	948	11	955	17	5.91%	0.43
	MOL1-20	0.07386	0.00156	1.77337	0.03718	0.17412	0.00219	0.05108	0.00095	1038	23	1036	14	1035	12	1007	18	0.29%	0.79
	MOL1-21	0.05936	0.00105	0.74046	0.01325	0.09046	0.00109	0.02691	0.00048	580	20	563	8	558	6	537	9	0.90%	0.18
	MOL1-22	0.06341	0.00131	0.85986	0.01765	0.09833	0.00122	0.06526	0.00218	722	23	630	10	605	7	1278	41	4.13%	0.04
	MOL1-23	0.05926	0.00108	0.73199	0.01336	0.08957	0.00108	0.03327	0.00064	577	20	558	8	553	6	662	13	0.90%	0.12
	MOL1-24	0.06025	0.00111	0.78393	0.01445	0.09436	0.00114	0.02713	0.00056	613	20	588	8	581	7	541	11	1.20%	0.11
	MOL1-25	0.06098	0.00121	0.81246	0.01605	0.09661	0.00119	0.02909	0.00052	639	22	604	9	595	7	580	10	1.51%	0.64
	MOL1-26	0.06065	0.00195	0.69007	0.02053	0.08252	0.00100	0.02545	0.00091	627	71	533	12	511	6	508	18	4.31%	0.07
	MOL1-27	0.06852	0.00122	1.27811	0.02299	0.13527	0.00162	0.04461	0.00077	884	19	836	10	818	9	882	15	2.20%	0.44
	MOL1-28	0.06200	0.00112	0.85807	0.01564	0.10037	0.00121	0.03116	0.00072	674	20	629	9	617	7	620	14	1.94%	0.05
	MOL1-29	0.06809	0.00120	1.08128	0.01923	0.11516	0.00138	0.03468	0.00065	871	19	744	9	703	8	689	13	5.83%	0.04
	MOL1-30	0.06657	0.00127	0.93742	0.01795	0.10212	0.00125	0.02664	0.00075	824	21	672	9	627	7	531	15	7.18%	0.07
	MOL1-31	0.05863	0.00133	0.70586	0.01591	0.08730	0.00110	0.02636	0.00051	553	28	542	9	540	7	526	10	0.37%	0.75
	MOL1-32	0.06020	0.00136	0.71163	0.01597	0.08572	0.00109	0.02556	0.00051	611	27	546	9	530	6	510	10	3.02%	0.62
	MOL1-33	0.06342	0.00115	0.86015	0.01570	0.09835	0.00118	0.02225	0.00042	722	20	630	9	605	7	445	8	4.13%	0.13
	MOL1-34	0.06915	0.00146	1.39992	0.02932	0.14681	0.00184	0.04447	0.00103	903	23	889	12	883	10	879	20	0.68%	0.26

(*continued on next page*)

Table 2 (*continued*)

River	Analysis (Sample No. and Spot No.)	CORRECTED RATIOS								CORRECTED AGES (Ma)									
		$^{207}Pb/^{206}Pb$	1σ	$^{207}Pb/^{235}U$	1σ	$^{206}Pb/^{238}U$	1σ	$^{208}Pb/^{232}Th$	1σ	$^{207}Pb/^{206}Pb$	1σ	$^{207}Pb/^{235}U$	1σ	$^{206}Pb/^{238}U$	1σ	$^{208}Pb/^{232}Th$	1σ	Degree of Discordance	Th/U
	MOL1-36	0.07003	0.00129	1.17720	0.02174	0.12189	0.00147	0.03749	0.00067	929	19	790	10	741	8	744	13	6.61%	0.44
	MOL1-37	0.07542	0.00147	1.65485	0.03230	0.15912	0.00196	0.04235	0.00078	1080	21	991	12	952	11	838	15	4.10%	0.86
	MOL1-39	0.07199	0.00141	1.41304	0.02767	0.14234	0.00175	0.04109	0.00078	986	21	894	12	858	10	814	15	4.20%	0.59
	MOL1-40	0.06599	0.00143	1.09156	0.02347	0.11996	0.00150	0.03708	0.00069	806	25	749	11	730	9	736	13	2.60%	1.28
	MOL1-41	0.05857	0.00123	0.72432	0.01510	0.08968	0.00111	0.02948	0.00102	551	25	553	9	554	7	587	20	0.18%	0.06
	MOL1-42	0.05879	0.00111	0.74648	0.01414	0.09207	0.00112	0.02672	0.00056	559	21	566	8	568	7	533	11	0.35%	0.08
	MOL1-44	0.05924	0.00111	0.72391	0.01366	0.08862	0.00107	0.02599	0.00049	576	21	553	8	547	6	519	10	1.10%	0.17
	MOL1-45	0.05932	0.00114	0.74408	0.01427	0.09097	0.00111	0.02642	0.00051	579	22	565	8	561	7	527	10	0.71%	0.21
	MOL1-46	0.05915	0.00114	0.70464	0.01357	0.08638	0.00105	0.02661	0.00051	573	22	542	8	534	6	531	10	1.50%	0.22
	MOL1-47	0.06124	0.00167	0.70291	0.01710	0.08324	0.00101	0.02565	0.00029	648	60	541	10	515	6	512	6	5.05%	0.19
	MOL1-48	0.06053	0.00154	0.70360	0.01763	0.08429	0.00110	0.02627	0.00060	623	32	541	11	522	7	524	12	3.64%	0.49
	MOL1-49	0.06188	0.00126	0.74848	0.01523	0.08772	0.00108	0.02699	0.00055	670	23	567	9	542	6	538	11	4.61%	0.35
	MOL1-50	0.06678	0.00298	1.14982	0.04897	0.12487	0.00167	0.03809	0.00043	831	95	777	23	759	10	756	8	2.37%	0.77
	MOL1-51	0.06564	0.00154	1.11867	0.02589	0.12358	0.00158	0.03741	0.00074	795	28	762	12	751	9	742	14	1.46%	1.60
	MOL1-53	0.06900	0.00139	1.22285	0.02456	0.12852	0.00159	0.03996	0.00078	899	22	811	11	779	9	792	15	4.11%	0.95
	MOL1-55	0.05924	0.00128	0.71853	0.01547	0.08795	0.00110	0.02685	0.00055	576	26	550	9	543	7	536	11	1.29%	0.48
	MOL1-56	0.06974	0.00141	1.23684	0.02485	0.12860	0.00159	0.04023	0.00079	921	22	817	11	780	9	797	15	4.74%	0.99
	MOL1-57	0.06684	0.00170	0.90265	0.02015	0.09794	0.00120	0.02987	0.00034	833	54	653	11	602	7	595	7	8.47%	0.13
	MOL1-58	0.06120	0.00149	0.72700	0.01748	0.08615	0.00111	0.02635	0.00066	646	30	555	10	533	7	526	13	4.13%	0.31
	MOL1-59	0.07133	0.00144	1.37243	0.02764	0.13952	0.00172	0.03016	0.00061	967	22	877	12	842	10	601	12	4.16%	0.42
	MOL1-60	0.17104	0.00345	10.66728	0.21451	0.45227	0.00561	0.12132	0.00250	2568	18	2495	19	2405	25	2314	45	6.78%	0.36
	MOL1-61	0.06918	0.00164	1.32224	0.03093	0.13860	0.00178	0.04216	0.00095	904	28	855	14	837	10	835	18	2.15%	0.47
	MOL1-62	0.05924	0.00150	0.76411	0.01910	0.09353	0.00122	0.00903	0.00054	576	32	576	11	576	7	182	11	0.00%	0.18
	MOL1-63	0.06934	0.00166	1.21729	0.02870	0.12731	0.00164	0.03892	0.00087	909	28	809	13	773	9	772	17	4.66%	0.54
	MOL1-64	0.06666	0.00181	1.18459	0.03162	0.12887	0.00174	0.03977	0.00105	827	33	793	15	781	10	788	20	1.54%	0.41
	MOL1-65	0.06703	0.00167	1.13792	0.02802	0.12311	0.00160	0.05183	0.00125	839	30	772	13	748	9	1021	24	3.21%	0.56
	MOL1-66	0.06437	0.00160	1.04065	0.02558	0.11723	0.00152	0.03566	0.00082	754	30	724	13	715	9	708	16	1.26%	0.52
	MOL1-67	0.06648	0.00162	1.23545	0.02961	0.13477	0.00175	0.03973	0.00090	822	29	817	13	815	10	787	17	0.25%	0.65
	MOL1-70	0.07048	0.00295	1.58121	0.06271	0.16271	0.00221	0.04934	0.00058	942	88	963	25	972	12	973	11	0.93%	0.56
	MOL1-71	0.07478	0.00165	1.40181	0.03072	0.13594	0.00172	0.04289	0.00094	1063	24	890	13	822	10	849	18	8.27%	0.55
	MOL1-72	0.06318	0.00279	0.95109	0.03982	0.10918	0.00152	0.03352	0.00041	714	96	679	21	668	9	666	8	1.65%	0.36
	MOL1-73	0.07193	0.00177	1.48786	0.03605	0.15000	0.00195	0.04753	0.00108	984	29	925	15	901	11	939	21	2.66%	0.71
	MOL1-74	0.07299	0.00162	1.72342	0.03797	0.17123	0.00217	0.04933	0.00109	1014	25	1017	14	1019	12	973	21	0.49%	0.50
	MOL1-76	0.07055	0.00198	1.17517	0.03239	0.12080	0.00164	0.03796	0.00099	944	34	789	15	735	9	753	19	7.35%	0.55
	MOL1-77	0.06108	0.00151	0.77418	0.01886	0.09192	0.00120	0.03004	0.00071	642	30	582	11	567	7	598	14	2.65%	0.53
	MOL1-78	0.06124	0.00151	0.73542	0.01786	0.08708	0.00113	0.02630	0.00071	648	30	560	10	538	7	525	14	4.09%	0.19
	MOL1-80	0.06060	0.00717	0.70777	0.08298	0.08470	0.00175	0.02571	0.00094	625	32	543	49	524	10	513	19	3.63%	1.72
	RV3C-01	0.06089	0.00095	0.58186	0.00806	0.06933	0.00049	0.02201	0.00018	636	33	466	5	432	3	440	4	7.78%	25.10
	RV3C-72	0.06458	0.00103	0.80484	0.01124	0.09038	0.00067	0.05180	0.00119	761	33	600	6	558	4	1021	23	7.49%	0.04
	RV3C-89	0.07669	0.00429	1.57802	0.08575	0.14923	0.00259	0.04786	0.00154	1113	57	962	34	897	15	945	30	7.24%	0.70
	RV3C-104	0.06704	0.00606	0.96445	0.08521	0.10434	0.00242	0.03122	0.00141	839	45	686	44	640	14	621	28	7.16%	0.73
	RV3C-02	0.06154	0.00215	0.65407	0.02199	0.07711	0.00077	0.02272	0.00018	658	73	511	14	479	5	454	4	6.73%	153.86
	RV3C-78	0.06364	0.00144	0.80152	0.01686	0.09134	0.00078	0.06150	0.01005	730	47	598	10	563	5	1206	12	6.09%	0.00
	RV3C-10	0.06739	0.00200	1.04908	0.02962	0.11292	0.00109	0.03490	0.00975	850	60	728	15	690	6	694	11	5.61%	0.01
	RV3C-73	0.06262	0.00693	0.76164	0.08245	0.08821	0.00238	0.02810	0.00154	695	78	575	48	545	14	560	30	5.50%	0.68
	RV3C-11	0.05944	0.00089	0.57795	0.00765	0.07051	0.00050	0.02262	0.00019	583	32	463	5	439	3	452	4	5.42%	22.17
	RV3C-09	0.06007	0.00183	0.61793	0.01798	0.07462	0.00070	0.02036	0.00017	606	64	489	11	464	4	407	3	5.30%	54.28
	RV3C-06	0.06186	0.00384	0.73120	0.04440	0.08574	0.00122	0.02681	0.00317	669	44	557	26	530	7	535	62	5.09%	0.11
	RV3C-67	0.06181	0.00236	0.73029	0.02677	0.08568	0.00099	0.02657	0.00088	668	80	557	16	530	6	530	17	5.06%	0.25
	RV3C-79	0.12048	0.00197	5.31035	0.07683	0.31965	0.00276	0.09318	0.00131	1963	29	1871	12	1788	13	1801	24	9.80%	0.44

(*continued on next page*)

Table 2 (*continued*)

River	Analysis (Sample No. and Spot No.)	CORRECTED RATIOS $^{207}Pb/^{206}Pb$	1σ	$^{207}Pb/^{235}U$	1σ	$^{206}Pb/^{238}U$	1σ	$^{208}Pb/^{232}Th$	1σ	CORRECTED AGES (Ma) $^{207}Pb/^{206}Pb$	1σ	$^{207}Pb/^{235}U$	1σ	$^{206}Pb/^{238}U$	1σ	$^{208}Pb/^{232}Th$	1σ	Degree of Discordance	Th/U
	RV3C-27	0.07475	0.00223	1.59245	0.04560	0.15446	0.00160	0.05524	0.00136	1062	59	967	18	926	9	1087	26	4.47%	0.31
	RV3C-76	0.06941	0.00711	1.23043	0.12322	0.12857	0.00355	0.03617	0.00295	911	69	815	56	780	20	718	58	4.46%	0.40
	RV3C-109	0.07018	0.00495	1.29555	0.08906	0.13389	0.00270	0.03932	0.00164	934	56	844	39	810	15	780	32	4.17%	0.66
	RV3C-60	0.10873	0.00306	4.33917	0.11592	0.28939	0.00359	0.09141	0.00215	1778	50	1701	22	1639	18	1768	40	8.53%	0.49
	RV3C-12	0.11618	0.00292	5.05995	0.12028	0.31587	0.00342	0.09017	0.00197	1898	45	1829	20	1770	17	1745	36	7.27%	0.54
	RV3C-64	0.06102	0.00123	0.75673	0.01392	0.08994	0.00072	0.02872	0.00312	640	43	572	8	555	4	572	61	3.04%	0.01
	RV3C-22	0.07317	0.00237	1.55909	0.04847	0.15451	0.00167	0.04676	0.00100	1019	64	954	19	926	9	924	19	3.01%	0.58
	RV3C-04	0.05997	0.00208	0.69721	0.02324	0.08435	0.00087	0.02508	0.00143	602	73	537	14	522	5	501	28	2.89%	0.09
	RV3C-34	0.05734	0.00084	0.54524	0.00744	0.06894	0.00049	0.02261	0.00024	504	32	442	5	430	3	452	5	2.82%	18.28
	RV3C-107	0.06065	0.00166	0.74629	0.01926	0.08924	0.00083	0.02572	0.00054	627	58	566	11	551	5	513	11	2.72%	0.31
	RV3C-07	0.06027	0.00312	0.72415	0.03657	0.08715	0.00110	0.02815	0.00278	613	21	553	22	539	7	561	55	2.67%	0.10
	RV3C-41	0.15265	0.00468	8.84874	0.26286	0.42036	0.00624	0.11697	0.00260	2376	51	2323	27	2262	28	2236	47	5.03%	1.27
	RV3C-97	0.07397	0.00240	1.63768	0.05068	0.16058	0.00181	0.04541	0.00116	1041	64	985	20	960	10	898	22	2.58%	0.39
	RV3C-23	0.06595	0.00176	1.09136	0.02774	0.11998	0.00111	0.03471	0.00343	805	55	749	13	731	6	690	67	2.56%	0.03
	RV3C-94	0.16009	0.00510	9.68649	0.30013	0.43883	0.00747	0.10483	0.00285	2457	53	2405	29	2345	33	2015	52	4.74%	0.89
	RV3C-18	0.06071	0.00309	0.75717	0.03757	0.09045	0.00118	0.04302	0.00555	629	32	572	22	558	7	851	5	2.54%	0.05
	RV3C-54	0.07285	0.00183	1.56181	0.03669	0.15547	0.00149	0.04629	0.00065	1010	50	955	15	932	8	915	12	2.53%	0.80
	RV3C-39	0.05982	0.01261	0.70336	0.14522	0.08526	0.00414	0.02521	0.00299	597	34	541	87	528	25	503	59	2.52%	0.57
	RV3C-74	0.18135	0.00330	12.15026	0.20367	0.48587	0.00527	0.12861	0.00279	2665	30	2616	16	2553	23	2445	50	4.41%	0.39
	RV3C-83	0.06707	0.00248	1.16851	0.04155	0.12635	0.00150	0.03740	0.00124	840	75	786	19	767	9	742	24	2.46%	0.27
	RV3C-59	0.11001	0.00176	4.62844	0.06498	0.30510	0.00255	0.08908	0.00115	1800	29	1754	12	1717	13	1725	21	4.84%	0.46
	RV3C-25	0.05894	0.00353	0.66609	0.03890	0.08194	0.00120	0.02513	0.00096	565	45	518	24	508	7	502	19	2.09%	0.45
	RV3C-106	0.06784	0.00232	1.24025	0.04064	0.13260	0.00150	0.04289	0.00087	864	69	819	18	803	9	849	17	2.03%	0.58
	RV3C-58	0.05999	0.00234	0.74104	0.02786	0.08958	0.00102	0.03283	0.00070	603	82	563	16	553	6	653	14	1.81%	0.51
	RV3C-85	0.06629	0.00360	1.14657	0.06050	0.12545	0.00189	0.03737	0.00077	815	10	776	29	762	11	742	15	1.80%	1.35
	RV3C-87	0.05990	0.00300	0.73733	0.03580	0.08928	0.00124	0.02521	0.00079	600	34	561	21	551	7	503	16	1.72%	0.49
	RV3C-81	0.06395	0.00447	0.99642	0.06794	0.11301	0.00215	0.03445	0.00090	740	43	702	35	690	12	685	18	1.71%	1.32
	RV3C-66	0.11349	0.00223	5.01326	0.09023	0.32033	0.00309	0.09301	0.00138	1856	35	1822	15	1791	15	1798	25	3.62%	0.63
	RV3C-08	0.07017	0.00583	1.41696	0.11548	0.14648	0.00280	0.04417	0.00262	933	45	896	49	881	16	874	51	1.69%	0.47
	RV3C-96	0.07325	0.00181	1.63756	0.03792	0.16214	0.00153	0.04682	0.00064	1021	49	985	15	969	8	925	12	1.67%	0.79
	RV3C-92	0.05863	0.00178	0.66580	0.01923	0.08235	0.00081	0.02565	0.00282	554	65	518	12	510	5	512	56	1.57%	0.02
	RV3C-43	0.05920	0.00381	0.70257	0.04425	0.08606	0.00139	0.02713	0.00091	575	34	540	26	532	8	541	18	1.52%	0.68
	RV3C-77	0.06769	0.00233	1.26094	0.04154	0.13510	0.00154	0.04647	0.01199	859	70	828	19	817	9	918	34	1.40%	0.01
	RV3C-98	0.06571	0.00225	1.12814	0.03693	0.12452	0.00137	0.02219	0.00134	797	70	767	18	757	8	444	26	1.36%	0.29
	RV3C-38	0.06859	0.00374	1.32911	0.07068	0.14051	0.00221	0.04708	0.00149	886	34	859	31	848	12	930	29	1.29%	0.63
	RV3C-16	0.05955	0.00970	0.74092	0.11923	0.09023	0.00256	0.02380	0.00369	587	45	563	70	557	15	475	73	1.08%	0.33
	RV3C-13	0.05861	0.00241	0.68369	0.02718	0.08459	0.00100	0.02916	0.00150	553	87	529	16	524	6	581	29	1.05%	0.11
	RV3C-52	0.05918	0.00277	0.72766	0.03294	0.08917	0.00114	0.02753	0.00076	574	99	555	19	551	7	549	15	0.84%	0.51
	RV3C-110	0.07081	0.00359	1.50955	0.07421	0.15463	0.00246	0.04255	0.00126	952	12	934	30	927	14	842	24	0.81%	0.73
	RV3C-21	0.11664	0.00382	5.42749	0.17052	0.33740	0.00461	0.09570	0.00278	1905	58	1889	27	1874	22	1847	51	1.66%	0.53
	RV3C-56	0.05854	0.00209	0.69554	0.02384	0.08616	0.00092	0.02990	0.00226	550	76	536	14	533	5	596	44	0.62%	0.05
	RV3C-71	0.07102	0.00185	1.54243	0.03770	0.15750	0.00152	0.04716	0.00076	958	52	948	15	943	8	931	15	0.49%	0.58
	RV3C-75	0.06713	0.00337	1.27206	0.06196	0.13742	0.00201	0.04386	0.00144	842	23	833	28	830	11	868	28	0.39%	0.46
	RV3C-26	0.06995	0.00410	1.47827	0.08422	0.15323	0.00261	0.04743	0.00143	927	23	922	35	919	15	937	28	0.27%	0.86
	RV3C-84	0.05850	0.00176	0.70621	0.02025	0.08756	0.00086	0.03079	0.00128	548	65	543	12	541	5	613	25	0.26%	0.09
	RV3C-49	0.05887	0.00167	0.73116	0.02024	0.09008	0.00085	0.03144	0.00193	562	61	557	12	556	5	626	38	0.22%	0.04
	RV3C-88	0.06965	0.00164	1.46535	0.03223	0.15258	0.00139	0.04464	0.00083	918	48	916	13	915	8	883	16	0.09%	0.34
	RV3C-62	0.05847	0.00347	0.71796	0.04137	0.08904	0.00142	0.02905	0.00213	548	34	550	24	550	8	579	42	0.05%	0.12
	RV3C-05	0.06353	0.00272	1.04706	0.04343	0.11957	0.00143	0.04828	0.00203	726	88	727	22	728	8	953	39	0.10%	0.18
	RV3C-46	0.05586	0.00318	0.55749	0.03102	0.07238	0.00108	0.01999	0.00025	446	33	450	20	451	6	400	5	0.13%	207.80

(*continued on next page*)

Table 2 (*continued*)

River	Analysis (Sample No. and Spot No.)	CORRECTED RATIOS								CORRECTED AGES (Ma)								Degree of Discordance	Th/U
		$^{207}Pb/^{206}Pb$	1σ	$^{207}Pb/^{235}U$	1σ	$^{206}Pb/^{238}U$	1σ	$^{208}Pb/^{232}Th$	1σ	$^{207}Pb/^{206}Pb$	1σ	$^{207}Pb/^{235}U$	1σ	$^{206}Pb/^{238}U$	1σ	$^{208}Pb/^{232}Th$	1σ		
	RV3C-102	0.07069	0.00271	1.55586	0.05755	0.15964	0.00196	0.04478	0.00144	948	77	953	23	955	11	885	28	0.21%	0.33
	RV3C-19	0.05845	0.00336	0.72323	0.04044	0.08972	0.00135	0.06864	0.01605	547	23	553	24	554	8	1342	45	0.23%	0.01
	RV3C-55	0.05789	0.00154	0.68926	0.01721	0.08634	0.00078	0.02642	0.00057	525	57	532	10	534	5	527	11	0.26%	0.25
	RV3C-30	0.05855	0.00728	0.73339	0.08979	0.09081	0.00228	0.02798	0.00302	551	45	559	53	560	13	558	59	0.32%	0.27
	RV3C-63	0.05722	0.00202	0.65232	0.02214	0.08268	0.00087	0.02367	0.00408	499	77	510	14	512	5	473	81	0.43%	0.02
	RV3C-28	0.05825	0.00225	0.71820	0.02690	0.08940	0.00099	0.02930	0.00254	539	83	550	16	552	6	584	50	0.43%	0.05
	RV3C-37	0.06672	0.00261	1.28645	0.04878	0.13980	0.00171	0.04300	0.00101	829	79	840	22	844	10	851	20	0.45%	0.68
	RV3C-93	0.06347	0.00231	1.06243	0.03708	0.12139	0.00139	0.03568	0.00048	724	75	735	18	739	8	709	9	0.49%	1.64
	RV3C-35	0.06298	0.00295	1.03339	0.04706	0.11896	0.00159	0.03455	0.00256	708	97	721	24	725	9	687	50	0.55%	0.11
	RV3C-42	0.05796	0.00300	0.70944	0.03584	0.08876	0.00126	-0.00299	0.00397	528	56	544	21	548	7	-61	81	0.69%	0.05
	RV3C-32	0.05803	0.00538	0.72032	0.06544	0.09000	0.00195	0.02646	0.00229	531	34	551	39	556	12	528	45	0.83%	0.28
	RV3C-61	0.06675	0.00228	1.30722	0.04273	0.14201	0.00160	0.03872	0.00306	830	70	849	19	856	9	768	60	0.83%	0.07
	RV3C-48	0.05806	0.00210	0.72633	0.02559	0.09073	0.00099	0.02836	0.00127	532	78	554	15	560	6	565	25	0.96%	0.13
	RV3C-47	0.05788	0.00146	0.71615	0.01763	0.08973	0.00079	0.02069	0.00158	525	55	548	10	554	5	414	31	0.99%	0.03
	RV3C-100	0.05699	0.00149	0.67097	0.01658	0.08539	0.00076	0.02534	0.00064	491	57	521	10	528	5	506	13	1.31%	0.19
	RV3C-86	0.06962	0.00333	1.54129	0.07162	0.16057	0.00237	0.04630	0.00164	917	96	947	29	960	13	915	32	1.34%	0.42
	RV3C-99	0.05672	0.00349	0.65961	0.03955	0.08435	0.00133	0.02446	0.00079	480	34	514	24	522	8	488	16	1.46%	0.62
	RV3C-103	0.06216	0.00303	1.02028	0.04817	0.11904	0.00169	0.03582	0.00179	680	23	714	24	725	10	711	35	1.50%	0.19
	RV3C-57	0.06348	0.00140	1.11401	0.02281	0.12725	0.00109	0.03968	0.00042	725	46	760	11	772	6	787	8	1.57%	0.95
	RV3C-44	0.07122	0.00450	1.67912	0.10352	0.17096	0.00315	0.05287	0.00234	964	21	1001	39	1017	17	1041	45	5.27%	0.50
	RV3C-40	0.06425	0.00393	1.18329	0.07060	0.13355	0.00228	0.03906	0.00088	750	24	793	33	808	13	774	17	1.89%	1.94
	RV3C-70	0.06748	0.00367	1.42900	0.07584	0.15357	0.00233	0.04576	0.00125	853	12	901	32	921	13	904	24	2.15%	0.77
	RV3C-90	0.05504	0.00245	0.60418	0.02601	0.07960	0.00098	0.02325	0.00079	414	23	480	16	494	6	465	16	2.81%	0.31
	RV3C-82	0.05624	0.00183	0.69732	0.02176	0.08992	0.00090	0.02639	0.00046	461	71	537	13	555	5	526	9	3.22%	0.62
	RV3C-105	0.05605	0.00217	0.68919	0.02576	0.08918	0.00099	0.02662	0.00073	454	84	532	15	551	6	531	14	3.34%	0.33
	RV3C-50	0.06820	0.00302	0.96219	0.04156	0.10232	0.00135	0.02810	0.00170	875	89	684	22	628	8	560	34	8.98%	0.18
	RV3C-31	0.05552	0.00273	0.68147	0.03270	0.08900	0.00116	0.02710	0.00090	433	34	528	20	550	7	541	18	3.98%	0.40

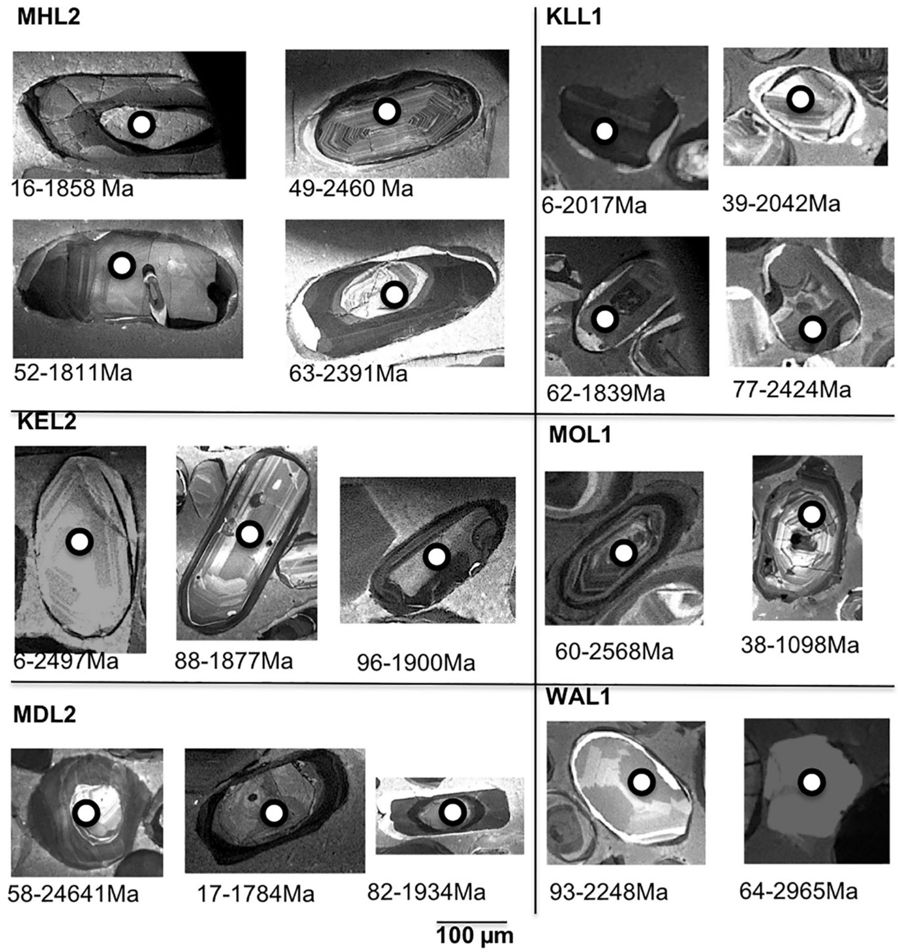

Fig. 3. Representative older grains of Mesoproterozoic to Archean zircons found in this study, from each river basin. The grain point number and the respective age are also given (analytical spot marked with a circle). Sample numbers are same as those in Fig. 1.

One hundred and sixty spots on 125 grains were analyzed. Grains younger than ~1.1 Ga closely plot on the concordia line (Fig. 4a). Zircons from Maha Oya are characterized by giving a majority of concordant ages. Major peaks at 560, 610, 780, 820 and 970 Ma are observed along with subordinate peaks between 1020 and 2400 Ma (Fig. 5f, h).

Most zircons have Th/U values > 0.1 (Fig. 7) consistent with their igneous origin. Also, the zircons which could have been derived from felsic sources are plotted above those from other igneous sources (Fig. 7a). Several different trends can be distinguished from the Th/U vs. U-Pb age diagram, and it could be attributed to different growth mechanisms as magmatic events prolonged in the Sri Lankan basement. Hence, clearly distinct zircon populations are visible: an older population with ages from Mesoproterozoic to Archean, and a younger population with ages of early Neoproterozoic to late Cambrian (Fig. 6). The younger population is also characterized by a group of zircons with homogenous and/or core-rim zoning texture in CL images and Th/U ratios < 0.1, indicating metamorphic origin (Figs. 3 and 7b). These grains characteristically plot in the range of ~500–650 Ma (Fig. 6). The early Neoproterozoic to late Cambrian zircons are characterized by variable Th/U ratios > 0.1 reaching values of ~3, whereas the Mesoproterozoic to Archean zircons could be distinguished by their relatively homogeneous Th/U ratios compared to the former (Fig. 7).

In general, on chondrite-normalized REE diagrams, most of the zircons have slightly fractionated, depleted light REE and enriched heavy REE patterns with variable positive Ce anomalies and negative Eu anomalies, although some zircons from Kalu Ganga and Maha Oya rivers display moderately enriched light REE patterns without a significant Ce anomaly (Fig. 8). The Neoproterozoic to late Cambrian zircons show slightly elevated overall REE abundances compared to the Mesoproterozoic to Archean zircon population. The metamorphic grains and rims/overgrowths display slightly flat REE (particularly heavy REE, though variable) patterns (Fig. 8).

6. Discussion

6.1. Detrital zircons as provenance indicators

In a single river sediment sample, the zircons may represent a variety of sources, such as mafic, felsic, intermediate or metamorphic rocks. In addition, once formed, the zircons may be reworked and recycled within the crust through various geological processes. In geochronology, the provenance of detrital zircons is interpreted based on the population distributions of U–Pb ages. The presence of particular age groups is a powerful indicator of the source area within the drainage system during or prior to the deposition of the sample (Rubatto, 2002). However, detrital zircons can be recycled from older sedimentary rocks, and potential source areas may contain several groups of different ages. Therefore, it is not simply possible to assign individual age groups to a specific source area. Hence, provenance analysis requires a thorough understanding of the distribution of primary bedrocks and sedimentary sources for the zircon grains in the target samples (e.g. Xiang et al., 2011; Iizuka et al., 2013b).

In elucidating zircon provenances, Th/U plays an important role.

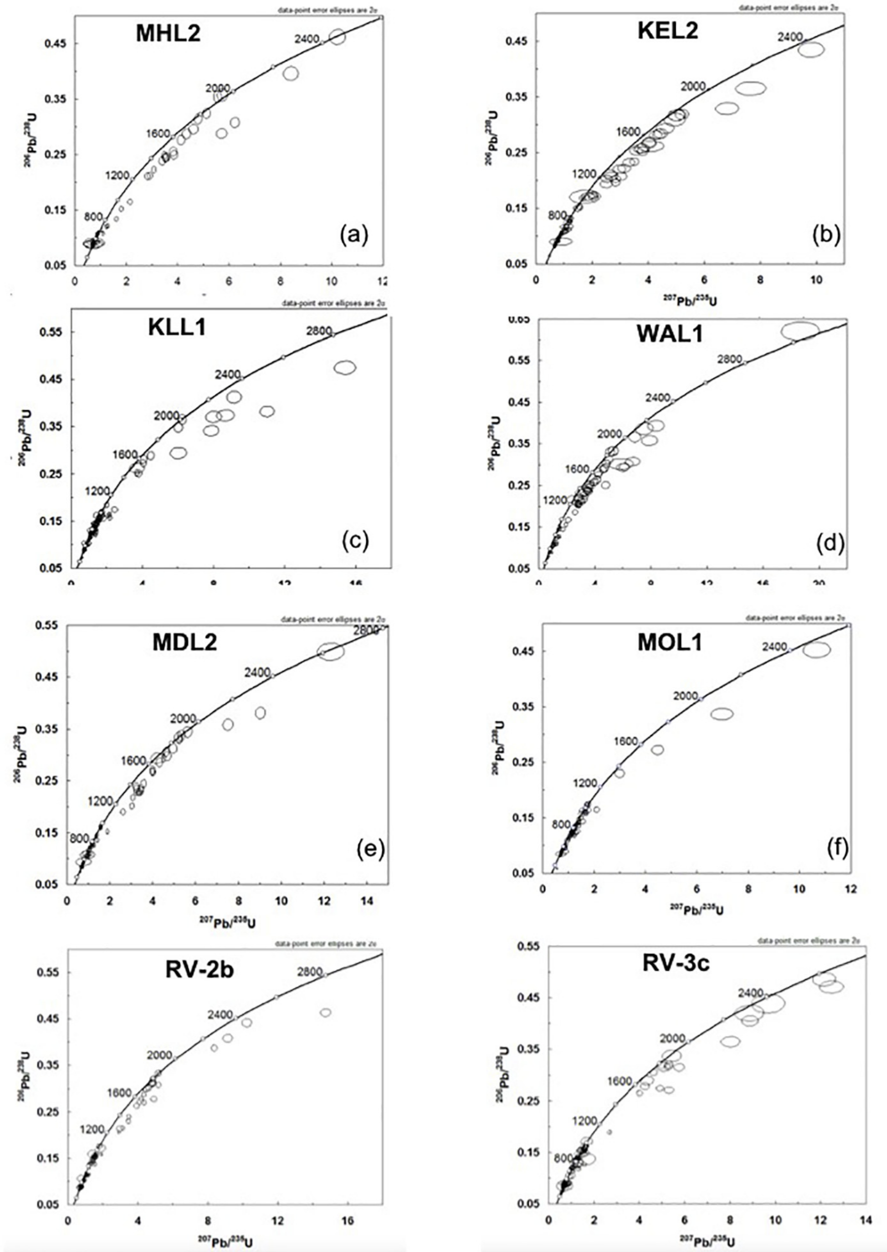

Fig. 4. Concordia diagrams of dated zircons from each of the major river basins of Sri Lanka. Sample numbers are same as those in Fig. 1.

The U and Th contents and Th/U ratios of magmatic zircon should promote higher Th contents relative to U contents at their crystallization, resulting in higher Th/U ratios for zircons in mafic to intermediate rocks than in felsic rocks (Kemp et al. 2006; Xiang et al., 2011; Iizuka et al., 2013a). However, when zircon crystallizes in disequilibrium with melt, U and Th are more easily able to enter the zircon lattice, and their contents and Th/U values depend mainly on the degree of disequilibrium (e.g. Wang et al., 2011a,b). On the other hand, Th/U values in metamorphic zircons is usually very low (typically below 0.1) due to availability of other common phases with differential geochemical affinities for U and Th (e.g. Rubatto, 2002). Hence, based on observations and experimental data (e.g. Wang et al., 2011a,b, Rubatto, 2002), the Th/U value of zircons is generally fixed as follows; felsic magmatic sources (> 1), mafic-intermediate magmatic sources (< 1, > 0.1) and metamorphic sources (< 0.1). Thus, the behavior of U and Th in zircon can be used as a geochemical indicator to determine their origins and crystallization environments (Rubatto, 2002; Xiang et al., 2011).

The Th/U ratios of our zircon samples are plotted in the Fig. 7. It is clear from this figure that majority of the zircons have Th/U > 0.1 and span in an age range from late Cambrian to late Proterozoic. Out of this group, more younger zircons (e.g. ca. < 1000 Ma old) are characterized with a variable Th/U ratio from 0.1 to 2.9 whereas the older grains have Th/U < ~1. The metamorphic zircons have Th/U ratio below 0.1, reaching very low values. Accordingly, distinct origins of sources as mafic to intermediate and felsic and metamorphic could be identified from the studied zircon population.

6.2. Zircon growth episodes displayed by Sri Lankan rivers

Out of the total population of zircons of each river, nearly 30% of the grains are represented by Mesoproterozoic to Archean zircons (> ~1100–3100 Ma). Most of these older grains are transparent in CL images and with rounded edges, having clear magmatic textures with oscillatory zoning (Figs. 2 and 3). These grain morphologies and textural patterns are consistent with Archean detrital zircons found

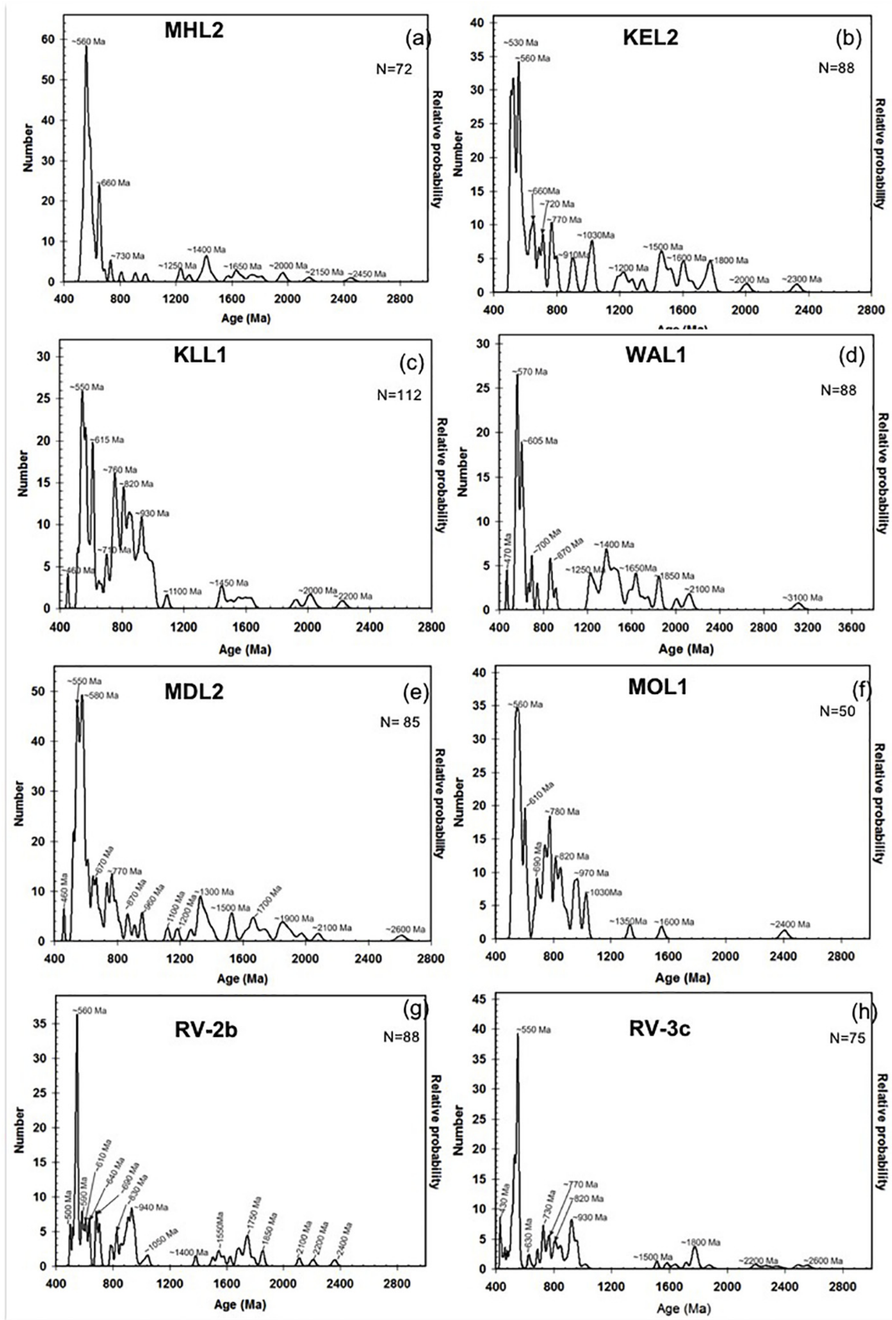

Fig. 5. Relative probability against U-Pb age for analyzed zircons of each river in this study, showing distribution of age peaks. Sample numbers are same as those in Fig. 1. See text for details.

elsewhere in the world (e.g. Su et al., 2011; Li et al., 2014; Chen et al., 2017; Sakyi et al., 2018), probably subjected to repeated crustal recycling, before they were trapped in the precursor rocks of the Sri Lankan lithotectonic units. In addition, they may have experienced multiphase reworking with exotic Archean sources.

The vast majority of the zircon population (~70%) from all rivers could be classified as Neoproterozoic to late Cambrian zircons (> ~430–1000 Ma). Of course, there is a minor population of zircons which falls in to the Silurian times as well (Fig. 6a). In this category, zircon grains belong to both igneous and metamorphic origin. In general, these 'younger' zircons are highly variable in shape compared to the older counterparts (Mesoproterozoic to Archean zircons). The magmatic zircons are clearly distinguished from those of metamorphic origin with respect to their morphology and internal textures, and also in terms of Th/U values (Fig. 7). Some of the grains were overgrown during the Neoproterozoic metamorphic activity by generating a clear mantle-rim domain over the early igneous core domain (Fig. 2).

Considering the overall age distribution data, the total zircon populations could be further subdivided into several narrow sub-groups, such as 480–680 Ma, 680–1000 Ma, 1100–1300 Ma, 1300–1700 Ma, 1700–1900 Ma, 2100–2300 Ma, 2300–2600 Ma. This could be seen in Fig. 6 and indicate that the crustal growth of Sri Lanka was not continuous and has been episodic since the Archean.

6.3. Regional provenance controls on the detrital zircons

6.3.1. Provenance implications of older zircon population

As mentioned above, Mesoproterozoic- to Archean-aged Zircons

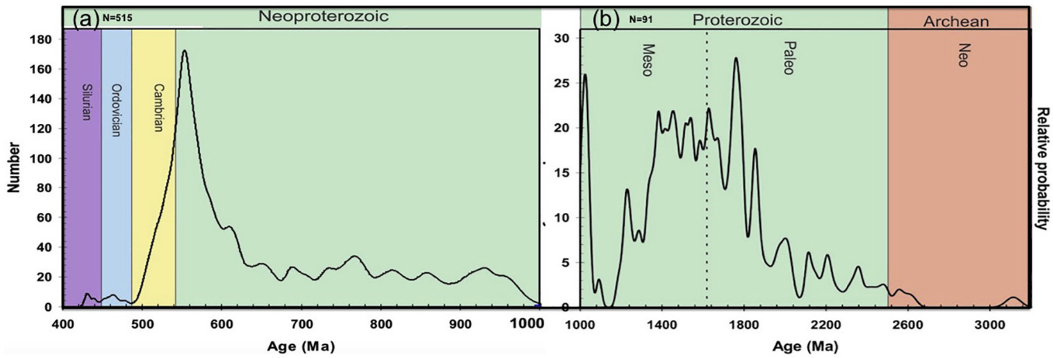

Fig. 6. Relative probability against U-Pb age for the entire zircon population dated in the present study, showing overall distribution of age peaks at different geological times. The total zircon ages could be distributed into several narrow groups, such as 480–680 Ma, 680–1000 Ma, 1100–1300 Ma, 1300–1700 Ma, 1700–1900 Ma, 2100–2300 Ma, 2300–2600 Ma, showing discontinuous crustal growth in Sri Lanka from Archean to late Cambrian. See text for details.

(> ~1100–3100 Ma) make up approximately 30% of the total age population with a prominent peak at 1.6–2 Ga (Fig. 6), which may be related to Meso to Paleoproterozoic HC, WC and KC rocks in the catchment of most of the rivers. The detrital zircons from the HC rocks indicate a widespread igneous intrusion event at 1.9 Ga, while Sm-Nd crustal residence ages of the HC and WC rocks are in the range of ~1.6–2 Ga (Milisenda et al. 1988, 1994; Hölzl et al., 1994). The zircon εHf values in metamorphosed rocks of the HC show variation from −20.5 to 1.6, with crustal model ages in the range of 1.5–2.8 Ga (Santosh et al., 2014; He et al., 2015). Zircons in charnockitic rocks also display a predominantly large negative εHf values ranging from −33.3 to −6.7, and older crustal model ages from 2 to 3.6 Ga (Santosh et al., 2014; He et al., 2015). These authors have suggested a mixed source comprising juvenile Neoproterozoic and reworked Mesoproterozoic – Archean components in the HC. In the Wanni Complex rocks, Sm–Nd crustal residence age peak at ~1.6 Ga is prominent, and markedly positive εHf values of the WC (from +5 to +15) suggest juvenile components as the source of the protoliths. The εHf values of samples from the KC range from slightly negative to positive, with crustal model ages mainly from 1.5 Ga to 1.8 Ga. This trend suggests its protoliths were derived from mantle sources with the input of minor reworked Neoarchean-Paleoproterozoic deep crustal sources. Particularly the Mahaweli and Kalu Rivers flow over a large part of the HC (Fig. 1) and the Mesoproterozoic and Archean zircons from these rivers have wider peaks at 1.2–2.5 Ga. Although both Kelani River and Maha Oya originate from the HC, they flow largely on the WC and KC. However, wide age peaks of Mesoproterozoic to Archean zircons in the Kelani River almost overlap with those shown by Mahaweli and Kalu Rivers which flow entirely over the HC (Fig. 1), despite the fact that the abundance of older zircon population in the Maha Oya river is less prominent (Fig. 5f). Hence, the older population of detrital zircons from the four rivers (Mahaweli, Kalu, Kelani and Maha Oya) probably indicates the same provenance. On the other hand, the Walawe and Maduru Oya Rivers flow over a wider area of the VC and their older zircons show more or less similar distribution pattern with a wider peak from 1.1 to 2.1 Ga. This could be a characteristic provenance indication with respect to the VC, although a minor fraction of the older zircons could be derived from the HC sources as well, probably as a result of tectonic mixture at the boundary between the HC and VC (Fig. 1).

6.3.2. *Provenance implications of younger zircon population*

As discussed above, ~70% of Neoproterozoic- to late Cambrian-aged zircon grains (~430–1000 Ma) accumulate with prominent peak ages at 530–670 Ma, 700–870 Ma and ~910–1030 Ma from all the rivers. This spectrum of ages is remarkably similar in all the rivers, displaying a pervasive zircon growth history related to Neoproterozoic magmatic events in the Sri Lankan terrane. This age distribution is particularly analogous to the trends found in lithologies in the Sri Lankan basement (e.g. Kröner and Williams, 1993; Kröner et al., 1991; Shiraishi et al. 1994; Hölzl et al., 1994; Kröner et al., 2013; Santosh et al., 2014; Dharmapriya et al., 2015; Takamura et al., 2016; He et al., 2016a,b). Hence, these magmatic pulses could be directly linked to the orogenic events of collision of the Wanni and Vijayan arcs, closing the HC paleo-ocean during the assembly of the Gondwana supercontinent (e.g. Shiraishi et al., 1994; Santosh et al., 2014).

6.3.3. *Metamorphic and metasomatic impacts on younger zircons*

Older populations (Mesoproterozoic to Archean) of zircons show unchanged Th/U evolution through time (Fig. 7), which we interpret to reflect a closed system behavior. One younger population shows a trend

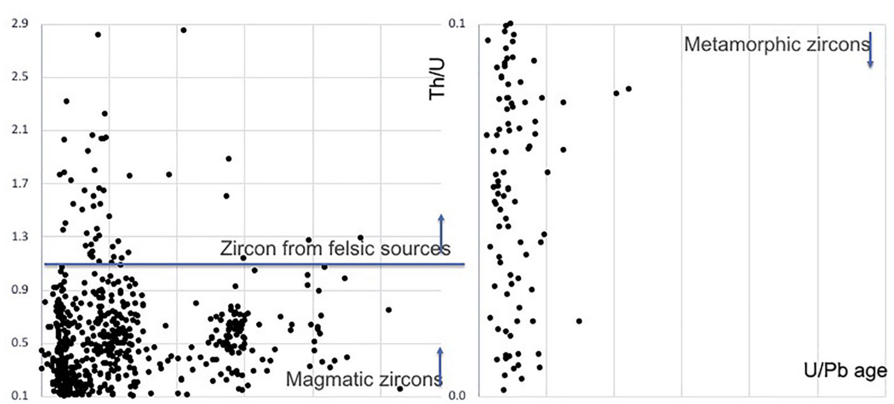

Fig. 7. Plot of Th/U vs. U/Pb age of the entire zircon population showing zircons derived from felsic, pure magmatic and metamorphic sources. See text for details.

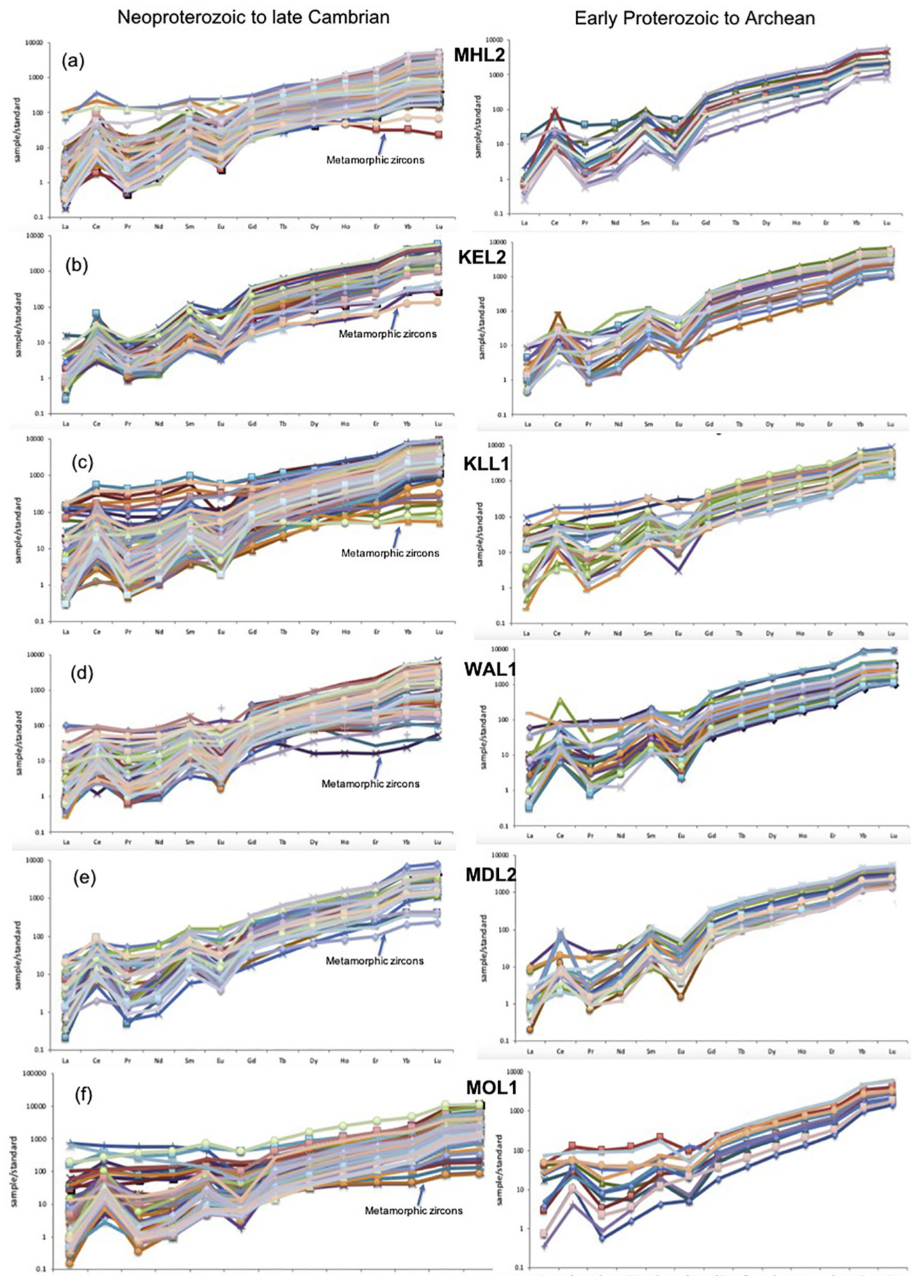

Fig. 8. Chondrite-normalized rare earth element (REE) patterns of dated zircons showing geochemical differences of Mesoproterozoic to Archean and Neoproterozoic to late Cambrian zircons. Note the slightly high overall REE levels of the younger age population and more-or-less flat heavy REE patterns of metamorphic zircons.

of lowering of the Th/U values, especially in overgrowths, which could indicate competition for Th with high Th minerals (monazite, allanite etc.) during their evolution. Late Neoproterozoic metamorphism may have affected these grains, lowering the Th/U values and paving the way for crystallization of a zircon population with typically low Th/U values (< 0.1). Thus, latest Neoproterozoic-Cambrian zircon population with distinctly low Th/U values (< 0.1) observed in all the river sand samples clearly represent high-grade metamorphism in the three lithologic complexes of Sri Lanka. In some of the Neoproterozoic grains, higher Th/U and could be interpreted to reflect open system behavior such as breakdown of minerals with high Th/U competition with high U minerals (e.g. xenotime), sedimentary components or metasomatic effects. Further, a negative Eu anomaly is usually attributed to the presence of Eu^{2+} in the melt since Eu^{2+} partitions less readily into zircon than Eu^{3+}. Many zircons exhibit both positive Ce and negative Eu anomalies, indicating both oxidised and reduced conditions during their formation (e.g. Hoskin and Schaltegger, 2003; Grimes et al., 2007).

6.3.4. Comparison with zircon data from various lithologies from Sri Lanka

Previous studies reported Mesoarchean to Paleoproterozoic ages for detrital zircon cores (3200–1800 Ma with peaks at 3200, 2900, 2400, 2000 Ma) from the HC (Hölzl et al., 1994; Kröner et al., 1987, 1994; Dharmapriya et al., 2016). Kitano et al. (2018) reported predominant Paleoproterozoic to Early Mesoproterozoic detrital zircon ages (ca. 2000–1500 Ma) from the eastern HC, and predominant Early to Mid-Neoproterozoic ages (ca. 1000–700 Ma) from the western part. Dharmapriya et al. (2016) and Takamura et al. (2016) reported Neoarchean to Paleoproterozoic (ca. 2800–1800 Ma) and Neoproterozoic (ca. 1000–700 Ma) ages of detrital zircons from the central HC. In the WC, the 916–980 Ma ages represent arc magmatism during early Neoproterozoic (Hölzl et al., 1994; Santosh et al., 2014). This was followed by the 805 Ma tonalitic magma emplacement in the WC. TheKC also bears more-or-less similar age spectrum. The 924–966 Ma ages from zircons of granitic gneisses and 617–770 Ma zircon ages from mafic rocks have records of magmatism in the VC. The metamorphic zircons from all the complexes mark ~550 Ma as a wide-spread overprinted event (Kröner et al., 1987, 1994; Hölzl et al., 1994; Santosh et al., 2014; He et al., 2016a,b).

Based on magmatic zircons in meta-igneous and meta-sedimentary rocks, several workers suggested that the Sri Lankan crustal basement likely contains considerable amounts of recycled Paleoproterozoic to Archean rocks (e.g. Santosh et al., 2014; Kröner et al., 2013; Takamura et al., 2016; Dharmapriya et al., 2015; Osanai et al., 2016; Malaviarachchi, 2016, 2018). Furthermore, the basement rocks in the Highland, Wanni and Vijayan complexes of Sri Lanka have whole-rock Nd and Hf model ages spanning from 2.65 to 2.87 Ga with an average of ca. 2.8 Ga (see review in Malaviarachchi, 2018). In this study, approximately 3–5% of zircons from each river were found to be between ~2.5 and ~3 Ga (Fig. 6). Detrital zircons with similar Archean ages are ubiquitous in all litho tectonic units of Sri Lanka, which are in the upstream of the studied rivers (Santosh et al., 2014; Kröner et al., 1987, 1991, 2003, 2013; He et al., 2015, 2016a,b; Takamura et al., 2016; Dharmapriya et al., 2015; Osanai et al., 2016). Therefore, we infer that the 2.8 Ga may be an important episode for the growth of juvenile crust and existence of an Archean basement in Sri Lanka.

Majority of zircons from these crustal units are of Neoproterozoic to Cambrian origin and formed during the magmatic and collisional events related to the Gondwana assembly (e.g. Santosh et al., 2014; Kröner et al., 1987, 1991, 2003, 2013; He et al., 2015, 2016a,b; Takamura et al., 2016; Dharmapriya et al., 2015; Osanai et al., 2016). Among the studied river sands, Neoproterozoic- to Cambrian-aged zircon grains constitute up to ~70% of the total age population with a peak at ~550 Ma (Fig. 6a). Rivers Mahaweli, Kelani Kalu and Maha Oya flow over the Highland and Wanni crustal blocks of Sri Lanka (Fig. 1), and the Walawe River mainly touches the Vijayan Complex crustal unit. Therefore, approximately similar age peak among the Neoproterozoic- to Cambrian-aged zircon grains could be related to the pervasive Neoproterozoic magmatic events in connection with the amalgamation of the Gondwana Supercontinent.

Zircons of river sands in this study showing distribution from Archean to Paleoproterozoic and Neoproterozoic to late Cambrian age peaks are consistent with zircons from of basement rocks known from petrological studies of Sri Lanka (Kröner et al., 1987, 1994; Hölzl et al., 1994; Santosh et al., 2014; Dharmapriya et al., 2015; Kitano et al., 2018; Takamura et al., 2016; He et al., 2016a,b; Osanai et al., 2016). However, late Mesoproterozoic to early Neoproterozoic age populations (ca. 1100–1000 Ma) reported in previous studies (Kröner et al., 2003; Willbold et al., 2004; Kitano et al., 2018; Dharmapriya et al., 2016), were not recorded as a prominent peak in our zircons (e.g. Figs. 5 and 6).

In summary, the zircon geochronological data from this study generally indicate that multiple phases of magmatic pulses with episodic addition of new crust and reworking of older crust in the Sri Lankan basement throughout the history. This is clearly seen as age peaks at 480–680 Ma, 680–1000 Ma, 1100–1300 Ma, 1300–1700 Ma, 1700–1900 Ma, 2100–2300 Ma, 2300–2600 Ma (Fig. 6). The older model ages from previous studies from Sri Lanka could be correlated to crustal components ubiquitously found in subducted sediments in the Wanni-Vijayan dual arc system. We therefore suggest that the overall age peaks at ~1800 Ma and 550 Ma date the major crust formation events in the Sri Lankan basement.

6.4. Tectonic implications

The transitional age span (between ~1.1 Ga and ~1.6 Ga) showing a quick increase of zircon population observed in our study could be interpreted as correspondent with the timing of the onset of subduction forming the Vijayan and Wanni arcs against a 'Highland Complex paleo-ocean' (Shiraishi et al., 1994; Santosh et al., 2014). This inference is also supported by previous geochronological studies which revealed derivation of higher amount of arc-related calc-alkaline and mafic lithologies in the Wanni (from 1.6 to 1.1 Ga) and Vijayan Complexes (from 1.1 to 0.9 Ga), particularly with close proximity to their boundaries with the HC (Kröner et al., 2002, 2013; Braun and Kriegsman, 2003; Willbold et al., 2004; Santosh et al., 2014, Takamura et al., 2016; He et al., 2016a,b; Wijeratne and Malaviarachchi, 2017).

The magmatic episodes ranging from the 1.1–1.6 Ga and 870–1000 Ma could be considered as Grenvillian (e.g. Kröner et al., 2003, Willbold et al., 2004; Li et al., 2014) and related to mark the beginning of the breakup of the Rodinia supercontinent. The widespread breakup of Rodinia occurred during 830–800 Ma (Li et al., 2014) and therefore it is evident that near-continuous magmatic pulses observed in this study at 820–870, 700–780 Ma could have a connection to the dispersal of Rodinia. Subsequently, collisions and metamorphism associated with the assembly of Gondwana during the late Neoproterozoic (Meert, 2003) are well reflected in the continuous age peaks of 605–610, 530–580 and 430–500 Ma. Thus, a regional provenance contribution from sources of Grenvillian and Gondwanan is evident in the entire Sri Lankan basement. Similar records of magmatic events have been found in the East Africa (e.g. Kröner et al., 2000) and in South India (Santosh et al., 1989; Braun and Kriegsman, 2003), implying Sri Lankan terranes were probably a part of the East Africa.

7. Conclusions

We draw the following conclusions from the geochronology of detrital zircons from the major rivers in the Sri Lankan basement.

(1) Two main zircon populations are distinguishable depicting a widespread magmatism: Mesoproterozoic to Archean (~30%; > 1100–3100 Ma) and Neoproterozoic to late Cambrian (~70%; > ~430–1000 Ma), adding substantial amount of juvenile crust to the Sri Lankan basement from Palaeoproterozoic to late Cambrian.
(2) The studied zircons provide evidence for intensive and episodic (both short-spanned and long-spanned) magmatic activities resolvable into fine groups at 480–680 Ma, 680–1000 Ma, 1100–1300 Ma, 1300–1700 Ma, 1700–1900 Ma, 2100–2300 Ma, 2300–2600 Ma and 2600–3100 Ma. These periods of magmatism are correspondent with principal episodes of global continental crustal growth, indicating most of the continental crust of Sri Lanka have formed in the Neoproterozoic. The older zircons may have mainly originated from the recycled ancient (Palaoproterozoic to Archean) crust.
(3) The change of the frequency of age peaks at ~1.1 Ga and ~1.6 Ga, giving rise to significant peaks in the Mesoproterozoic might reflect triggering of subduction in a paleo tectonic setting, forming the Wanni and Vijayan dual arc system, respectively.

Acknowledgements

U-Pb dating was financially supported by the National Key R & D Program of China (2017YFC0601306) and National Natural Science Foundation of China (41522203). Financial support from National Research Council of Sri Lanka Grant No. NRC-15-089 for field work is gratefully acknowledged. Preleminary analytical preparations of zircons in Sri Lanka and laboratory work in India were generously supported by Indo-Sri Lanka bilateral research project under Ministry of Science, Technology and Research, Sri Lanka (Grant No. MTR/TRD/AGR/3/2/20) and Department of Science and Technology, India (Grant No. DSTO/CEAS/SJK/1802). Ms. P.G. Athira of the Indian Institute of Science, Bangalore, Ms. Chen Chen, IGGCAS of the Chinese Academy of Science, Beijing and Mr. Wang Yu of the China University of

Geoscience, Beijing are especially thanked for helps in zircon seperation, making zircon grain mounts and LA-ICPMS analytical assistance, respectively. Prof. M. Satish-Kumar is thanked for providing necessary facilities at Niigata University, Japan for the first author to finalyse the manuscript during a collaborative stay. Authors are also thankful for positive comments by Prof. Guochun Zhao on a previous version of the manuscript, two anonymous reviewers and the handling Editor Dr. Manoj Pandit for improving the manuscript.

Appendix A. Supplementary material

Supplementary data associated with this article can be found, in the online version, at https://doi.org/10.1016/j.jseaes.2018.08.029.

References

Alizai, A., Carter, A., Clift, P.D., Van Laningham, S., Williams, J.C., Kumar, R., 2011. Sediment provenance, reworking and transport processes in the Indus River by U-Pb dating of detrital zircon grains. Global Planet. Change 76, 33–55.

Andersen, T., 2002. Correction of common lead in U-Pb analyses that do not report 204Pb. Chem. Geol. 192, 59–79.

Amidon, W.H., Burbank, D.W., Gehrels, G.E., 2005. Construction of detrital mineral populations: insights from mixing of U-Pb zircon ages in Himalayan rivers. Basin Res. 17, 463–485.

Baur, N., Kröner, A., Todt, W., Liew, T.C., Hofmann, A.W., 1991. U-Pb isotopic systematics of zircons from prograde and retrograde transition zones in high grade orthogneisses, Sri Lanka. J. Geol. 99, 527–545.

Berger, A.R., Jayasinghe, N.R., 1976. Precambrian structure and chronology in the Highland Series of Sri Lanka. Precambr. Res. 3, 559–576.

Black, L.P., Kamo, S.L., Allen, C.M., Aleinikoff, J.N., Davis, D.W., Korsch, R.J., Foudoulis, C., 2003. TEMORA 1: a new zircon standard for Phanerozoic U-Pb geochronology. Chem. Geol. 200, 155–170.

Braun, I., Kriegsman, L.M., 2003. Proterozoic crustal evolution of southernmost India and Sri Lanka. In: In: Yoshida, M., Windley, B.F., Dasgupta, S. (Eds.), Proterozoic east Gondwana: Supercontinent Assembly and Breakup, vol. 206. Geological Society of London Special Publication, pp. 169–202.

Burton, K.W., O'Nions, R.K., 1990. The timescale and mechanism of granulite forma- tion at Kurunegala, Sri Lanka. Contribut. Mineral. Petrol. 106, 66–89.

Chen, Y., Yan, M., Fang, X., Song, C., Zhang, W., Zan, J., Zhang, Z., Li, B., Yang, Y., Zhang, D., 2017. Zircon U-Pb geochronological and sedimentological study of the Simao Basin, Yunnan: Implications for the Early Cenozoic evolution of the Red River. Earth Planet. Sci. Lett. 476, 22–33.

Condie, K.C., Belousova, E., Griffin, W.L., Sircombe, K.N., 2009. Granitoid events in space and time: constraints from igneous and detrital zircon age spectra. Gondwana Res. 15 (3–4), 228–242.

Condie, K.C., Bickford, M.E., Aster, R.C., Belousova, E., Scholl, D.W., 2011. Episodic zircon ages, Hf isotopic composition, and the preservation rate of continental crust. Geol. Soc. Am. Bull. 123 (5–6), 951–957.

Cooray, P.G., 1962. Charnockites and their associated gneisses in the Precambrian of Ceylon. J. Geol. Soc. London 118, 239–273.

Cooray, P.G., 1984. An introduction to the geology of Sri Lanka. National Museum Sri Lanka Publication, pp. 340.

Cooray, P.G., 1994. The Precambrian of Sri Lanka: a historic review. Precambr. Res. 66, 3–18.

De Maesschalck, A.A., Oen, I.S., Hebeda, E.H., Verschure, R., Arps, E.S., 1990. Rb- Sr whole rock ages of Kataragama and Pottuvil Charnockites and east Vijayan gneiss: indication of a 2 Ga metamorphism in the highlands of south east Sri Lanka. J. Geol. 98, 772–779.

Deng, K., Shouye, Y., Chao, L., Su, N., Bi, L., Chang, Y., Chang, S., 2017. Detrital zircon geochronology of river sands from Taiwan: Implications for sedimentary provenance of Taiwan and its source link with the east China mainland. Earth Sci. Rev. 164, 31–47.

Dharmapriya, P.L., Malaviarachchi, S.P.K., Santosh, M., Lang, L., Sajeev, K., 2015. Late-Neoproterozoic ultrahigh-temperature metamorphism in the Highland Complex, Sri Lanka. Precambr. Res. 271, 311–333.

Dharmapriya, P.L., Malaviarachchi, S.P.K., Sajeev, K., Zhang, Chengli, 2016. New LA-ICPMS U-Pb ages of detrital zircons from the Highland Complex: Insights into Late Cryogenian to Early Cambrian (ca. 665–535 Ma) linkage between Sri Lanka and India. Int. Geol. Rev. 58, 1856–1883.

Dharmapriya, P.L., Malaviarachchi, S.P.K., Kriegsman, L.M., Galli, A., Sajeev, K., Zhang, C., 2017. New constraints on the P-T path of HT/UHT metapelites from the Highland Complex of Sri Lanka. Geosci. Front. 8, 1405–1430.

Fernando, G.W.A.R., Dharmapriya, P.L., Baumgartnerc, L.P., 2017. Silica-undersaturated reaction zones at a crust–mantle interface in the Highland Complex, Sri Lanka: mass transfer and melt infiltration during high-temperature metasomatism. Lithos 284, 237–256.

Grimes, C.B., John, B.E., Kelemen, P., Mazdab, F., Wooden, J., Cheadle, M.J., Hanghøj, K., Schwartz, J., 2007. Trace element chemistry of zircons from oceanic crust: A method for distinguishing detrital zircon provenance. Geology 35, 643–646.

Hapuarachchi, D.J.A.C., 1968. Cordierite and wollastonite-bearing rocks of south- west of Ceylon. Geol. Mag. 105, 317–324.

Hatherton, T., Pattiarachchi, D.B., Ranasinghe, V.V.C., 1975. Gravity map of Sri Lanka 1:1,000,000. Geological Survey Department, Sri Lanka, Professional Paper 3, pp. 39.

Hawkesworth, C.J., Dhuime, B., Pietranik, A.B., Cawood, P.A., Kemp, A.I.S., Storey, C.D., 2010. The generation and evolution of the continental crust. J. Geol. Soc. 167 (2), 229–248.

Hawkesworth, C.J., Cawood, P.A., Dhuime, B., 2013. Continental growth and the crustal record. Tectonophysics 609, 651–660.

He, X.-F., Santosh, M., Tsunogae, T., Malaviarachchi, S.P.K., 2015. Early to late Neoproterozoic magmatism and magma mixing–mingling in Sri Lanka: implications for convergent margin processes. Gondwana Res. https://doi.org/10.1016/j.gr.2015.02.013.

He, X.F., Santosh, M., Tsunogae, T., Malaviarachchi, S.P.K., Dharmapriya, P.L., 2016a. Neoproterozoic arc accretion along the 'eastern suture' in Sri Lanka during Gondwana assembly. Precambr. Res. 279, 57–80.

He, X.F., Santosh, M., Tsunogae, T., Malaviarachchi, S.P.K., 2016b. Early to late Neoproterozoic magmatism and magma mixing–mingling in Sri Lanka: Implications for convergent margin processes during Gondwana assembly. Gondwana Res. 32, 151–180.

Hiroi, Y., Ogo, Y., Namba, K., 1994. Evidence for prograde metamorphic evolution of Sri Lankan pelitic granulites, and implications for the development of continental crust. Precambr. Res. 66, 245–263.

Hiroi, Y., Yanagi, A., Kato, M., Kobayashi, T., Prame, B., Hokada, T., Satish-Kumar, M., Ishikawa, M., Adachi, T., Osanai, Y., Motoyoshi, Y., Shiraishi, K., 2014. Super cooled melt inclusions in lower-crustal granulites as a consequence of rapid exhumation by channel flow. Gondwana Res. 25, 226–234.

Hölzl, S., Hofmann, A.W., Todt, W., Köhler, H., 1994. U-Pb Geochronology of the Sri Lankan basement. Precambrian Res. 66, 123–149.

Hoskin, P.W.O., Schaltegger, U., 2003. The composition of zircon and igneous and metamorphic petrogenesis. Rev. Mineral. Geochem. 53, 27–62.

Iizuka, T., Hirata, T., Komiya, T., Rino, S., Katayama, I., Motoki, A., Maruyama, S., 2005. U-Pb and Lu–Hf isotope systematics of zircons from the Mississippi River sand: implications for reworking and growth of continental crust. Geology 33 (6), 485–488.

Iizuka, T., Campbell, I.H., Allen, C.M., Gill, J.B., Maruyama, S., Makoka, F., 2013a. Space and time: constraints from igneous and detrital zircon age spectra. Gondwana Res. 15 (3–4), 228–242.

Iizuka, T., Campbell, I.H., Allen, C.M., Gill, J.B., Maruyama, S., Makoka, F., 2013b. Evolution of the African continental crust as recorded by U-Pb, Lu-Hf and O isotopes in detrital zircons from modern rivers. Geochim. Cosmochim. Acta 107, 96–120. https://doi.org/10.1016/j.gca.2012.12.028.

Kemp, A.I.S., Hawkesworth, C.J., Paterson, B.A., Kinny, P.D., 2006. Episodic growth of the Gondwana supercontinent from hafnium and oxygen isotopes in zircon. Nature 439, 580–783.

Kitano, I., Osanai, Y., Nakano, N., Adachi, T., Fitzsimons, I.C.W., 2018. Detrital zircon and igneous protolith ages of high-grade metamorphic rocks in the Highland and Wanni Complexes, Sri Lanka: Their geochronological correlation with southern India and East Antarctica. J. Asian Earth Sci. 156, 122–144.

Kleinschrodt, R., 1994. Large-scale thrusting in the lower crustal basement of Sri Lanka. Precambr. Res. 66, 39–57.

Köhler, H., Dratch, V., Hölzl, S., Fehr, T., 1991. Geochronology of Sri Lanka basement -Part II: Rb-Sr and Sm-Nd dating on mineral and whole rock samples. Terra Abstr. 3, 504.

Kriegsman, L., 1995. The Pan-African events in East Antarctica: a review from Sri Lanka and the Mozambique Belt. Precambr. Res. 75, 263–277.

Kröner, A., Jaeckel, P., Williams, I.S., 1994. Pb-loss patterns in zircons from a high-grade metamorphic terrain as revealed by different dating methods: U-Pb and Pb-Pb ages for igneous and metamorphic zircons from northern Sri Lanka. Precambrian Res. 66, 151–181.

Kröner, A., Kehelpannala, K.V.W., Hegner, A., 2003. Ca. 750–1100 Ma magmatic events and Grenville-age deformation in Sri Lanka: relevance for Rodinia supercontinent formation and dispersal, and Gondwana amalgamation. J. Asian Earth Sci. 22, 279–300.

Kröner, A., Cooray, P.G., Vitanage, P.W., 1991. Lithotectonic subdivision of the Precambrian basement in Sri Lanka. Geological Survey Department, Sri Lanka, Professional Paper 5, pp. 5–21.

Kröner, A., Hegner, E., Collins, A.S., Windly, B.F., Brewer, T.S., Razakamannana, T., Pidgeon, R.T., 2000. Age and magmatic history of the Antonanarivo block, central Madagascar, as derived from zircon geochronology and Nd isotopic systematics. Am. J. Sci. 300, 251–288.

Kröner, A., Rojas-Agramonte, Y., Kehelpannala, K.V.W., Zack, T., Hegner, E., Geng, H.Y., Wong, J., Barth, M., 2013. Age, Nd–Hf isotopes, and geochemistry of the Vijayan Complex of eastern and southern Sri Lanka: a Grenville-age magmatic arc of unknown derivation. Precambr. Res. 234, 288–321.

Kröner, A., Williams, I.S., 1993. Age of metamorphism in the high-grade rocks of Sri Lanka.

Kröner, A., Williams, I.S., Compston, W., Baur, N., Vithanage, P.W., Perera, L.R.K., 1987. Zircon ion microprobe dating of high grade rocks in Sri Lanka. J. Geol. 95, 775–791.

Li, X.-H., Li, Z.-X., Li, W.-X., 2014. Detrital zircon U-Pb age and Hf isotope constraints on the generation and reworking of Precambrian continental crust in the Cathaysia Block, South China: a synthesis. Gondwana Res. 25 (3), 1202–1215.

Ludwig, K.R., 2003. ISOPLOT: a plotting and regression program for radiogenic-isotope data. U.S. Geological Survey Open-File Report, 39.

Malaviarachchi, S.P.K., Takasu, A., 2011. Electron microprobe dating of monazites from Sri Lanka. J. Geol. Soc. Sri Lanka 14, 81–90.

Malaviarachchi, S.P.K., 2016. A concise review on new Lu-Hf and U-Pb isotope systematics of metamorphosed magmatic rocks of Sri Lanka: insights into recent geotectonic models. J. Geol. Soc. Sri Lanka 17, 101–112.

Malaviarachchi, S.P.K., 2018. Review on age of magmatism and crust formation in Sri Lanka: U-Pb and Lu–Hf isotopic perspectives. J. Indian Inst. Sci. 1–11. https://doi.org/10.1007/s41745-018-0069-1.

Mathavan, V., Fernando, G.W.A.R., 2001. Reactions and textures in grossular- wollastonite-scapolite calc-silicate granulites from Maligawila, Sri Lanka. Lithos 59, 217–232.

Mathavan, V.W.K.B.N., Prame, W.K.B.N., Cooray, P.G., 1999. Geology of the high-grade Proterozoic terrains of Sri Lanka and the assembly of Gondwana: an update on recent developments. Gondwana Res. 2, 237–250.

Meert, J.G., 2003. A synopsis of events related to the assembly of eastern Gondwana. Tectonophysics 362, 1–40.

Milisenda, C.C., 1991. Compositional characteristics of the Vijayan Complex. Professional Paper No. 5. Geological Survey Department, Sri Lanka, pp. 135–140.

Milisenda, C.C., Leiw, T.C., Hofmann, A.W., Kohlerr, H., 1994. Nd isotopic mapping of the Sri Lanka basement: update, and additional constraints from Sr isotopes. Precambr. Res. 66, 95–110.

Milisenda, C.C., Leiw, T.C., Hofmann, A.W., Kröner, A., 1988. Isotopic mapping of age provinces in Precambrian high grade terrains: Sri Lanka. J. Geol. 96, 608–615.

Osanai, Y., Sajeev, K., Nakano, N., Kitano, I., Kehelpannala, W.K.V., Kato, R., Adachi, T., Malaviarachchi, S.P.K., 2016. UHT granulites of the Highland Complex of Sri Lanka II: Geochronological constraints and implications for Gondwana correlation. J. Mineral. Petrol. Sci. 111, 157–169.

Perera, L.R.K., 1987. Petrogenesis of Granulite-Facies Metamorphic Rocks in Sri Lanka. M.Phil. Thesis, University of Peradeniya (unpublished).

Perera, L.R.K., 1984. Co-existing cordierite-almandine – a key to the metamorphic history of Sri Lanka. Precambr. Res. 25, 349–364.

Pohl, J.G., Emmermann, R., 1991. Chemical composition of the Sri Lanka Precambrian Basement. Geological Survey Department, Sri Lanka, Professional Paper 5, pp. 94–123.

Prame, W.K.B.N., 1991. Metamorphism and nature of the granulite facies crust in south western Sri Lanka: Characterization by pelitic/psammopelitic rocks and associated granulites. Geological Survey Department, Professional Paper 5, Sri Lanka, pp. 188–200.

Raase, P., Schenk, V., 1994. Petrology of granulite facies metapelites of the Highland Complex, Sri Lanka: implication for the metamorphic zonation and the P-T path. Precambr. Res. 66, 265–294.

Rino, S., Kon, Y., Sato, W., Maruyama, S., Santosh, M., Zhao, D., 2008. The Grenvillian and Pan-African orogens: world's largest orogenies through geologic time, and their implications on the origin of superplume. Gondwana Res. 14 (1–2), 51–72.

Rubatto, D., 2002. Zircon trace element geochemistry: partitioning with garnet and the link between U-Pb ages and metamorphism. Chem. Geol. 184, 123–138.

Sakyi, P.A., Su, B.X., Kwayisi, D., Chen, C., Bai, Y., Alemayehu, M., 2018. Zircon trace element constraints on the evolution of the Paleoproterozoic Birimian granitoids of the West African Craton (Ghana). J. Earth Sci. 29, 43–56.

Sandiford, N., Powell, R., Martin, S.F., Perera, L.R.K., 1988. Thermal and baric evolution of garnet granulites from Sri Lanka. J. Metamorph. Geol. 6, 351–364.

Santosh, M., Iyer, S.S., Vasconelloe, M.B.A., Enzweiller, J., 1989. Late Precambrian alkaline plutons in south west India: geochronologic and rare-earth element constraints on Pan-African metamorphism. Lithos 24, 65–79.

Santosh, M., Tsunogae, T., Malaviarachchi Sanjeewa, P.K., Zhang, Z.M., Ding, H.X., Tang, L., Dharmapriya, P.L., 2014. Neoproterozoic crustal evolution in Sri Lanka: insights from petrologic, geochemical and zircon U–Pb and Lu–Hf isotopic data and implications for Gondwana assembly. Precambrian Res. 255, 1–29.

Schumacher, R., Shenk, V., Raase, P., Vithanage, P.W., 1990. Granulite facies metamorphism of metabasic and intermediate rocks in the Highland Series of SriLanka. In: Ashworth, J.R., Brown, M. (Eds.), High Temperature Metamorphism and Crustal Anatexis. The Mineralogical Society series 2, pp. 235–271.

Shiraishi, K., Ellis, D.J., Hiroi, Y., Fanning, C.M., Motoyoshi, Y., Nakai, Y., 1994. Cambrian orogenic belt in east Antarctica and Sri Lanka: implications for Gondwana assembly. J. Geol. 102, 47–65.

Song, S.G., Zhang, L.F., Niu, Y.L., Su, L., Jian, P., Liu, D.Y., 2005. Geochronology of diamond-bearing zircons from garnet peridotite in the North Qaidam UHPM belt, Northern Tibetan Plateau: a record of complex histories from oceanic lithosphere subduction to continental collision. Earth Planet. Sci. Lett. 234, 99–118.

Song, S.G., Su, L., Li, X.-H., Zhang, G., Niu, Y.L., Zhang, L.F., 2010. Tracing the 850-Ma continental flood basalts from a piece of subducted continental crust in the North Qaidam UHPM belt, NW China. Precambr. Res. 183, 805–816.

Su, B.X., Qin, K.Z., Sakyi, P.A., Li, X.H., Yang, Y.H., Sun, H., Tang, D.M., Liu, P.P., Xiao, Q.H., Malaviarachchi, S.P.K., 2011. U-Pb ages and Hf-O isotopes of zircons from Late Paleozoic mafic-ultramafic units in southern Central Asian Orogenic Belt: tectonic implications and evidence for an Early-Permian mantle plume. Gondwana Res. 20, 516–531.

Takamura, Y., Tsunogae, T., Santosh, M., Malaviarachchi, S.P.K., Tsutsumi, Y., 2016. U-Pb geochronology of detrital zircons in metasediments of Sri Lanka: Implications for the regional correlations of Gondwana fragments. Precambr. Res. 281, 434–452.

Vitanage, P.W., 1985. Tectonics and mineralization in Sri Lanka. Bull. Geol. Soc. Finland 57, 157–168.

Voll, G., Kleinschrodt, R., 1991. Sri Lanka: Structural, magmatic and metamorphic development of a Gondwana fragment. Geological Survey Department Professional Paper 5, Sri Lanka, pp. 22–52.

Wang, C.Y., Campbell, I.H., Stepanov, A.S., Allen, C.M., Burtsev, I.N., 2011a. Growth rate of the preserved continental crust: II. Constraints from Hf and O isotopes in detrital zircons from Greater Russian Rivers. Geochim. Cosmochim. Acta 75, 1308–1345.

Wang, C.Y., Campbell, I.H., Allen, C.M., Williams, I.S., Eggins, S.M., 2009. Rate of growth of the preserved North American continental crust: evidence from Hf and O isotopes in Mississippi detrital zircons. Geochim. Cosmochim. Acta 73, 712–728.

Wang, X., Griffin, W.L., Chen, J., Huang, P., Li, X., 2011b. U and Th contents and Th/U ratios of zircon in felsic and mafic magmatic rocks: improved zircon-melt distribution coefficients. Acta Geol. Sin. 85, 164–174.

Wiedenbeck, M., Alle, P., Corfu, F., Griffin, W.L., Meier, M., Oberli, F., Vonquadt, A., Roddick, J.C., Speigel, W., 1995. Three natural zircon standards for U-Th–Pb, Lu–Hf, trace-element and REE analyses. Geostandard Newslett. 19, 1–23.

Wijeratne, A.M.G.K., Malaviarachchi, S.P.K., 2017. Preliminary geochemistry of Pottuvil Charnockites, Sri Lanka. J. Geol. Soc. Sri Lanka 18, 101–113.

Willbold, M., Hegner, E., Kleinschrodt, R., Stosch, H.-G., Kehelpannala, K.V.W., Dulski, P., 2004. Geochemical evidence for a Neoproterozoic magmatic continental margin in Sri Lanka-relevance for the Rodinia-Gondwana super continental cycle. Precambr. Res. 130, 185–198.

Xiang, W., Griffin, W.L., Jie, C.H., Pinyun, L., 2011. U and Th contents and Th/U ratios of zircon in felsic and mafic magmatic rocks: improved zircon-melt distribution coefficients. Acta Geol. Sin. 85, 164–174.

Xu, Y., Wang, C.Y., Zhao, T., 2016. Using detrital zircons from river sands to constrain major tectono-thermal events of the Cathaysia Block, SE China. J. Asian Earth Sci. 124, 1–13.

Yang, J., Gao, S., Chen, C., Tang, Y.Y., Yuan, H.L., Gong, H.J., Xie, S.W., Wang, J.Q., 2009. Episodic crustal growth of North China as revealed by U-Pb age and Hf isotopes of detrital zircons from modern rivers. Geochim. Cosmochim. Acta 73, 2660–2673.

Yuan, H.L., Gao, S., Liu, X.M., Li, H.M., Gunther, D., Wu, F.Y., 2004. Accurate U-Pb age and trace element determinations of zircon by laser ablation-inductively coupled plasma mass spectrometry. Geostandard Newslett. 28, 353–370.

Zheng, H., Clift, P.D., Wang, P., Tada, R., Jia, J., He, M., Jourdan, F., 2013. Pre-Miocene birth of the Yangtze River. Proc. Natl. Acad. Sci. 110 (19), 7556–7561.